A Luminance Noise Approach to Target Post-Receptor Visual Pathways; Application to Optic Nerve Disease

BY
CIERRA MICHELLE HALL
B.S., University of Illinois at Chicago, 2011

THESIS

Submitted as partial fulfillment of the requirements
for the degree of Doctor of Philosophy in Bioengineering
in the Graduate College of the
University of Illinois at Chicago, 2016

Chicago, IL

Defense Committee:

J. Jason McAnany, Ophthalmology and Visual Sciences, Advisor
Thomas Royston, Chair
Dingcai Cao, Ophthalmology and Visual Sciences
James Patton
John Hetling

ACKNOWLEDGEMENTS

Firstly, I would like to thank my PI Dr. J. Jason McAnany for his scientific tutelage, research advice, and for allowing me to use his lab space and equipment throughout the duration of my thesis research. The completion of my thesis and PhD would not have been possible without this generosity. I would also like to sincerely thank my other committee members – Dr. Royston, committee chair, Dr. Dingcai Cao, Dr. James Patton, and Dr. John Hetling – for all of their support, advice, and guidance through this process.

Many people provided assistance during the hundreds of hours of data collection for the experiments described hereafter, including Shu Wang for her excellent MATLAB programming skills, and Reema Bhagat for helping to conduct some of the initial experiments for Aim 1. I would also like to sincerely thank my generous lab mate Hansa Kundra and my patient and kind husband Brian Henry, for their donation of many hours of their time to my work, and for the many subjects and patients whose data was pivotal for the completion of this work.

I would also acknowledge support that I received through a CCTS PECTS scholarship 2015-2016, and full support from the Bioengineering department that I received during my first year of graduate studies.

Lastly, I am very grateful for the advice and support provided by friends throughout this process. There are too many to name, but some are: Vidyani Suryadevara, Jorjethe Roca, Veronica Arreola, Brynne Nicolsen, Monika Aggrawal, Julie Engh, Natalie Santiago, Amanda Rios, Natalie Petrovich, and many more.

CMH

TABLE OF CONTENTS

TABLE OF CONTENTS (Contd..)

TABLE OF CONTENTS (Contd..)

LIST OF TABLES

LIST OF FIGURES

LIST OF ABBREVIATIONS

AMD	**Age-related Macular Degeneration**
ANOVA	**Analysis of Variance**
C	**Contrast**
cd	**Candela**
CPD	**Cycles per Degree**
CPL	**Cycles per Letter**
CS	**Contrast Sensitivity**
CT	**Contrast Threshold**
CSF	**Contrast Sensitivity Function**
DEG	**Degree**
E_t	**Signal Energy at Threshold**
HVF	**Humphrey Visual Field**
k	**Sampling Efficiency**
L	**Luminance**
LAM	**Linear Amplifier Model**
LGN	**Lateral Geniculate Nucleus**
LOG	**Logarithm**
m	**Meter**
MAR	**Minimum Angle of Resolution**
MC	**Magnocellular**
ms	**Milliseconds**

LIST OF ABBREVIATIONS (Contd..)

MS	**Multiple Sclerosis**
NSD	**Noise Spectral Density**
Neq	**Equivalent Noise**
ON	**Optic Neuritis**
PC	**Parvocellular**
RMS	**Root Mean Square**
RP	**Retinitis Pigmentosa**
s	**Second**
SNR	**Signal to Noise Ratio**
t	**Time**

SUMMARY

Contrast sensitivity (CS), which is the ability to detect small differences in luminance, is a fundamental task of the visual system and loss of CS is an important marker for many disease states. Although clinically-applicable methods are available to assess CS, there are limitations to these standard methods. For example, they are unable to determine which of the two primary post-receptor visual pathways, the magnocellular (MC) and parvocellular (PC) pathways, mediates CS for a given task. Furthermore, standard clinical measures of CS cannot provide insight into mechanisms underlying CS abnormalities.

In this thesis, a test of CS using letter stimuli will be developed and applied to address these issues. To permit the development of this new CS test, the following series of questions will first be resolved and an optimized CS test will then be applied to patients who have optic nerve dysfunction to better understand their CS deficits. Question 1: Which optotypes should be used in tests of letter CS? Letters are relatively complex targets that are not all equally identifiable. Aim 1 will define the optimal letter set for use in CS testing. Question 2: Can luminance noise, defined as decrements and increments of luminance added to a stimulus (e.g. 'tv snow'), be used to target the MC and PC pathways? Although there is preliminary evidence that the temporal characteristics of noise can be manipulated to target these post receptor pathways selectively, the specific characteristics of noise needed to do so have not been fully defined. Aim 2 will determine the spatial and temporal characteristics of noise capable of targeting the MC and PC pathways. Question 3: What is the optimal letter size for use in targeting the MC and PC pathways using static and dynamic luminance noise? Aim 3 will determine the range of letter sizes that can be used to target selectively the MC and PC pathways. Question 4: What is the optimal letter duration for use in targeting the MC and PC pathways in

noise-based CS tests? Aim 4 will evaluate the ability of static and dynamic noise to target the MC and PC pathways across a series of letter exposure durations. Once the test is developed and finalized, it will be applied in Aim 5 to a small sample of patients who have optic neuritis (ON); the results from the patients will be compared to visually-normal control subjects.

Thus, this dissertation will develop a clinically applicable, noise-based test of letter CS that can independently assess function within the MC and PC pathways. This will permit evaluating potential deficits within the MC and PC pathways, as well as provide preliminary insight into potential factors that limit CS in patients who have ON.

I. INTRODUCTION

A. Problem Statement and Motivation

CS is an important and basic function of the visual system, and is defined as the ability to perceive small differences in luminance. CS is typically measured in the clinic using letter targets; however, the complexities of standard letter CS tests are not well appreciated. For example, letters contain a broad range of features (e.g. edges, general shape) any of which could potentially be used to identify the letter target and mediate CS. The information contained in the letter that is used for identification can be measured and quantified as in terms of "object frequency" in units of cycles per letter (cpl). Different object frequencies mediate CS under different conditions **(Hall et al., 2014; McAnany & Alexander, 2008)**, and different subjects may utilize different object frequencies under the same stimulus conditions.

As a further complication to CS measurements, there are two primary post-receptor processing streams that can mediate CS: the MC and PC pathways. The pathway that mediates performance affects CS and the object frequencies used for letter identification **(McAnany & Alexander, 2008)**. Consequently, for a complete understanding of letter CS, it is important to consider the object frequency information mediating CS and to assess performance independently within the MC and PC pathways. White visual luminance noise is a promising, but not routinely used, tool that may be useful for controlling the pathway that mediates letter CS, and this luminance noise approach will form the basis of the methodology used in this thesis.

In order to develop a noise-based test of letter CS for application to patient populations, a series of 4 unresolved problems in CS testing must first be addressed. **Problem 1**: the optimal set of optotypes for use in noise-based letter CS testing is not known. Aim 1 will resolve this gap in knowledge by measuring and comparing contrast threshold for individual letters in the presence

and absence of external white luminance noise using letters from the Sloan set. **Problem 2**: The spatio-temporal characteristics of luminance noise necessary for targeting the MC and PC pathways selectively have not been defined. Aim 2 will resolve this gap in knowledge by altering the spatial and temporal characteristics of external white noise and measuring contrast threshold for the letter set defined in Aim 1. **Problem 3**: The optimal letter size to be used in tests of letter CS in noise is unknown. Aim 3 will determine if the MC and PC pathways can be targeted for letters of different size and will define the optimal range of letter size for use in noise-based CS testing. **Problem 4**: The effect of stimulus duration on our ability to target the MC and PC pathways in noise is unknown. Stimulus duration will be manipulated in Aim 4 to determine if the proposed noise-based test can target the MC and PC pathways for a range of stimulus durations.

Lastly, after resolving these four fundamental issues, an optimized noise-based test of letter CS will be developed and applied to a small sample of patients who have optic nerve dysfunction (Aim 5). Previous work suggests that MC pathway CS is selectively affected in patients who have optic neuritis (ON) **(Cao et al., 2011)**. Therefore, the goal of Aim 5 is to provide preliminary data regarding the nature and extent of visual pathway abnormalities in patients who have ON. In addition to providing insight into MC and PC pathway CS in patients with ON, the test will also permit measurement of the 'internal noise' of the visual system **(Legge et al., 1987),** which may provide an explanation for the CS losses in these patients.

B. <u>Significance of the Study</u>

Currently, clinically applicable letter tests of CS that can selectively target the MC and PC pathways are not available. Furthermore, existing clinically-applicable CS tests are unable to estimate the amount of noise within the visual pathway ("internal noise"), which may provide

explanations for CS losses. The proposed test of letter CS that will be developed will resolve these issues by allowing for: 1) the independent assessment of function within the MC and PC post-receptor pathways, 2) greater flexibility of test parameters such as stimulus duration, and 3) estimation of internal noise levels.

II. BACKGROUND

A. Description of Contrast Sensitivity and its Measurement

CS is an important measure of visual function and is defined as the ability to discern the difference between luminances. Contrast (C) is commonly defined as the Weber fraction:

$$C = \frac{L_L - L_B}{L_B}, \quad (1)$$

where L_L is the luminance of the target and L_B is the background luminance that the target is presented on. In the case of standard letter stimuli, L_L is the luminance of the letter in units of candela per meter^2 (cd/m^2) and L_B is the background luminance in cd/m^2. Weber contrast is typically used for targets with one polarity (e.g. black stimulus on a white background). The present thesis will exclusively use Weber contrast, but there are other methods of defining contrast that are used for targets that have two polarities. Although these other definitions will not be used in this thesis, they are presented here for completeness. Michelson contrast is defined as:

$$C = \frac{L_{\max} - L_{\min}}{L_{\max} + L_{\min}}, \quad (2)$$

where $L_{\max}$ is the maximum luminance of the stimulus and $L_{\min}$ is the minimum stimulus luminance. Michelson contrast is commonly used for more complex stimuli that have areas of light and dark, such a sine wave grating (discussed further below).

Lastly, contrast in natural images, such as photos of scenery, is usually defined as RMS contrast:

$$C = \frac{L_\mu}{L_\sigma}, \quad (3)$$

where L_μ is the mean luminance of the image and L_σ is the standard deviation in luminance in the image. Elsewhere throughout this thesis, contrast (*C)* will refer to Weber contrast because of the use of letter stimuli. CS, is the reciprocal of contrast threshold (CT), where threshold is defined as the minimum amount of luminance necessary to differentiate the target (e.g. letter) from the background:

$$CS = \frac{1}{CT} \qquad (4)$$

The use of CS as a measure of visual function has a long history, with some of the earliest systematic studies performed by Pierre Bouguer using a simple apparatus of a candle and the shadow of a rod projected onto a white screen **(Bouguer, 1760)**. He determined that the contrast needed to differentiate the rod's shadow from the background reliably was 1.6% (i.e. the CT). The physicist Masson later calculated that his own and several observers' CT was about 1% and basically independent of the absolute luminance level **(Masson, 1845)**. He suggested that CT may be useful as a diagnostic quantity for doctors treating visual disorders. In 1890, Gustav Fechner reported that CT is approximately 1% for a wide range of conditions and stimuli **(Fechner, 1860; republished 1966)**, a value that was later corroborated over a hundred-fold range of luminance and a sixteen-fold range of size **(Zhang et al, 1989)**. Thus, early work is in general agreement that the minimum perceivable difference between two luminance levels (CT) is approximately 1%.

Letters: Letter optotypes have also be used to measure CS. Letters are broadband stimuli and contain many different spatial frequencies, as opposed to sine wave gratings that contain a single frequency (discussed further below). Low spatial frequencies correspond to general shape information, and high frequencies represent edge information or the 'outline' of the letter. Although the modern English alphabet contains 26 different letters, only a subset of these

characters, “the Sloan letter set,” is commonly used in vision testing. The Sloan set consists of 10 upper-case letters (C, D, H, K, N, O, R, S, V, Z) that were originally selected to be similarly identifiable in tests of visual acuity **(Sloan, 1959)**.

Letter charts for assessing CS were not available widely until the 20th century, despite the relatively widespread use of letter charts for visual acuity measurement **(Snellen, 1862)**. The first attempt at the creation of a letter CS chart was made by Ole Bull by painting dark gray letters on a black background **(Bull, 1881)**. Bjerrum then made letter charts with gray and black letters on white backgrounds with precise contrasts of 9, 20, 30, and 40 percent contrast, which he used at various light levels and with patients with eye diseases **(Bjerrum, 1884)**.

George Berry adapted Bjerrum’s charts for ‘light-difference’ (CS) measurements to study the effects of retrobulbular neuritis **(Berry, 1889)**, and as a result he found letters of 9% contrast the most useful for low contrast acuity testing. This is consistent with some modern charts such as the Regan low-contrast acuity charts **(Regan, 1988)**. Carsten Edmund later created a large letter chart with nine contrasts ranging from 1 to 100% with logarithmic spacing of contrast steps **(Edmund, 1924)**.

Pelli-Robson Chart: The Pelli-Robson chart, which uses letters of a constant size that vary in contrast, is currently the gold standard for clinical CS testing. Fig 1 shows an example of the Pelli-Robson chart that presents letters that decrease in contrast from left to right, and from top to bottom. The faintest letters that can be correctly identified provide a measure of CS **(Pelli et al., 1988)**.

Fig 1, Pelli-Robson letter CS chart **(Pelli et al., 1988)**

Sine Wave Gratings: Gratings of sinusoidal luminance modulation have also been used to measure CS. The use of these stimuli in vision science was pioneered by Selwyn and Schade **(Selwyn, 1948; Schade, 1956)**. Sinusoidal gratings are a series of light and dark bars, with one dark bar and one light bar composing one 'cycle', as seen in Fig. 2, below.

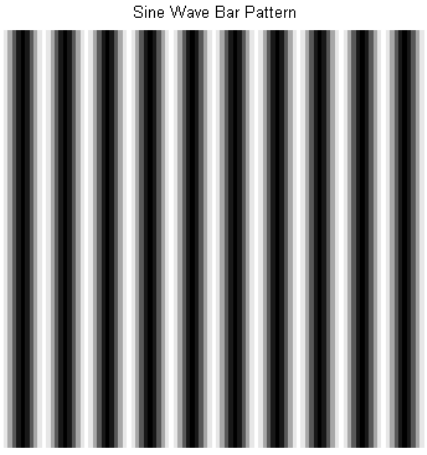

Fig 2, Sine wave pattern of periodic light and dark bars.

The formula for these waves is as follows:

$$\theta = a \cdot \sin(f \cdot x), \qquad (5)$$

where Θ is the function output, a is the amplitude of the wave, f is the frequency, and x is spatial location. The frequency is the inverse of wavelength, which is defined as follows in Eq. 6:

$$f = \frac{1}{\lambda}, \qquad (6)$$

where λ is the wavelength (typically in degrees of visual angle). As such, high spatial frequencies correspond to small wavelengths (narrow bars) and vice versa. Since this stimulus contains only one frequency in space, its Fourier spectrum is as simple as possible, containing only one frequency. The downside to these stimuli is that in identification tests, a subject can only say which way the stimulus is oriented (generally horizontal or vertical), as opposed to letters, where one may have up to 26 options in the alphabet, and 10 options for the Sloan letter set. The more alternatives a subject has, the less likely he/she will guess correctly at random, which increases the accuracy of the identification measurement.

Gabor Patches: Gabor patches are sine wave gratings windowed by a Gaussian envelope **(Gabor, 1946)**, shown below in Fig. 3. These stimuli are commonly used in vision science because they give the grating a circular bound and allow for the edges to taper off in contrast to eliminate abrupt edges.

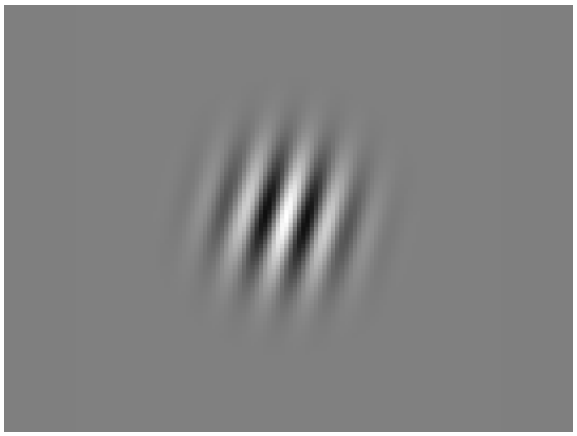

Fig 3, Gabor patch: sinusoidal pattern of light and dark bars, constrained by a gradual, circular envelope.

A novel approach to testing contrast threshold (and therefore CS) was pioneered by E. W. H. Selwyn, who used several sine wave gratings of different spatial frequency to examine contrast threshold in human subjects. In this manner, Selwyn discovered that there is a basic relationship between contrast threshold and the frequency of the sine wave gratings. For high frequency gratings (thinly interleaved bars of black and white), threshold was high, whereas for low frequency gratings (larger bands of black and white), threshold was low **(Selwyn, 1948)**. Selwyn generated sine wave gratings through photographic techniques, but Schade later refined the technique by using electronics and cathode ray tubes to produce finer control of the grating stimuli (**Schade, 1956**). Schade also more thoroughly investigated CS as a function of spatial frequency through systematic measurements of human CS based on his experience with television systems.

Campbell and Robson were the first to completely map CS across a broad range of grating spatial frequencies (**Campbell and Robson, 1968).** The resulting function that related CS to spatial frequency was termed the contrast sensitivity function (CSF). Shortly afterward, the

examination of CSFs of patients with ocular disease became more widespread, since measuring CSFs with sine wave gratings provided a systematic and precise measure. Attempts to create a CS chart using gratings were made, but were met with obstacles. Geoffrey Arden produced a CS chart with gratings by having cards printed with variable frequency vertical gratings, where the bottom of the card had low contrast, and the top of the card transitioned to a high contrast. The subject was shown the covered card, and then the covering was slid upward gradually revealing the higher contrasts. The subject indicated the point at which grating became detectable **(Arden, 1978)**. Unfortunately, the measurements proved insufficiently reliable among visually-normal subjects.

Arthur Ginsburg developed an improved CS chart using gratings that also used a variable frequency and contrast arrangement, but instead of using one continuous presentation of changing contrast, he used single, discrete patches of gratings of a certain frequency and contrast **(Ginsburg, 1984)**. In addition, he incorporated different orientations, increasing the number of alternative choices available to the patient, and therefore decreasing the number of correct guesses. Although the methodology was more precise, the test time was lengthy and therefore not convenient clinically. In more recent times, sine wave gratings have somewhat fallen out of favor and letter contrast sensitivity charts have been used more frequently.

B. <u>Object Frequency in Letter Identification</u>

Unlike Gabor patches, which have limited frequency content, letters and other natural stimuli contain a broad range of spatial frequencies. An example to illustrate the broadband nature of letters is shown below in Fig 4. The unfiltered letter at the left contains all of the object frequencies that are naturally present in the letter. A cosine log band-pass filter **(Peli, 1990)** was

applied to the unfiltered N to permit decomposition into four distinct frequency bands that are contained within the original letter (the figure shows center frequencies ranging from 0.65 to 10 cpl). In this way, it is possible to examine specific bands of spatial frequency information present in the broadband image. The broadband nature of the letter leads to the possibility that the subject could use any of the frequency information contained in the letter to identify it. This is particularly a concern for individuals with ocular dysfunction, who may use different information to identify letters compared to visually-normal subjects.

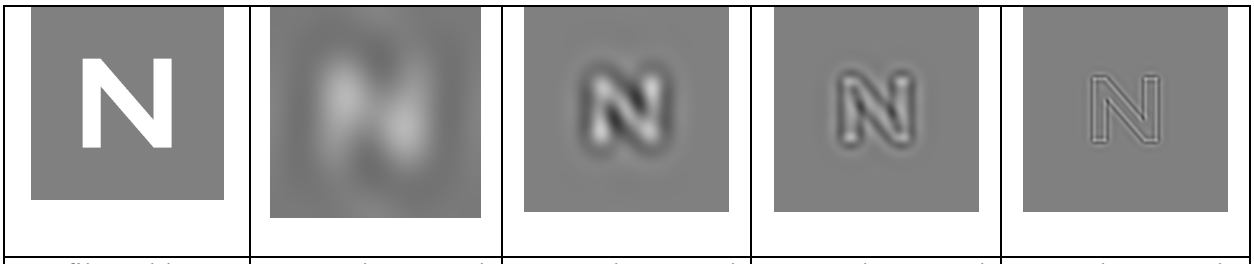

Unfiltered letter 'N'	0.65 cpl centered band-pass	1.88 cpl centered band-pass	3.75 cpl centered band-pass	10 cpl centered band-pass

Fig 4, Letter N unfiltered and filtered into various frequency bands (centered at the value below each image) using a band-pass filter.

Although the information mediating letter CS is not considered in standard clinical tests, letter object frequency has been studied extensively under laboratory conditions **(Alexander et al., 1994; Solomon and Pelli, 1994; Chung et al., 2002; Majaj et al., 2002; McAnany and Alexander, 2008; Oruc and Landy, 2009; Alexander and McAnany, 2010)**. The standard approach for studying the object frequency information mediating visual acuity and contrast sensitivity for letters has been to remove or mask selected object frequencies contained in the letter, and then measure the effect on performance. That is, if removing a range of object frequencies does not affect performance, then those frequencies must not be necessary for the

task. Conversely, if removing a range of object frequencies impairs performance, then those frequencies must be useful for performing the task.

Two distinct approaches based on this logic have been used to identify the object frequencies mediating letter CS: a letter filtering approach **(Alexander et al., 1994; Chung et al., 2002; McAnany and Alexander, 2008; Alexander and McAnany, 2010)** and a noise masking approach (i.e., "critical-band noise masking"; **Solomon and Pelli, 1994; Majaj et al., 2002; Oruc and Landy, 2009**). The former approach involves selectively removing object frequencies from the letter by spatial filtering, whereas critical-band noise masking attenuates the usefulness of selected object frequencies by masking them with spatially filtered luminance noise.

Despite differences in approach, previous studies that have examined the effect of letter size on the object frequencies mediating contrast sensitivity are in good agreement. For example, the data of Chung et al., who used band-pass filtered letters, indicate that a linear function with a slope of approximately 1/3 describes the relationship between log object frequency and log letter size, for letters of approximately 0.10 to 1.4 log MAR **(Chung et al., 2002)**. Similarly, the data of Majaj et al., who used critical-band noise masking **(Majaj et al., 2002)**, indicate that a linear relationship with a slope of approximately 1/3 can describe the relationship between log object frequency and log letter stroke frequency, for letter sizes of approximately 0.3 to 2.8 log MAR. We compared the two approaches directly for the first time by using 1) filtered letters presented against a uniform field and 2) unfiltered letters presented in filtered luminance noise and showed that the two conditions were equivalent for most letter sizes **(Hall et al., 2014)**.

C. Effect of Disease on CS

There are a number of studies examining the effect of disease on CS. The following is a brief review of CS in patients with various ophthalmic diseases.

Amblyopia: Freedman et al. found that CS was decreased over the entire range of spatial frequencies tested using sine wave gratings **(Freedman et al, 1975)**. Hess et al. found that, using sine wave gratings, some subjects exhibited decreased CS at all spatial frequencies, whereas other patients had CS loss only at intermediate and high frequencies **(Hess et al., 1976)**.

Age-related Macular Degeneration (AMD): Sjostrand et al., used sine wave gratings to evaluate CS in patients who have AMD. They found a marked decrease in CS for intermediate to high spatial frequencies in these patients **(Sjöstrand et al., 1977)**. Kleiner et al. found a loss of CS in patients with AMD, as assessed with the Ginsberg grating CS chart. These patients had CS losses for high spatial frequencies and for frequencies near the peak of the CSF **(Kleiner et al., 1988)**.

Retinitis Pigmentosa (RP): Lindberg et al. used sine wave grating plates to test CS in patients with RP. Although the patients had decreased CS at all spatial frequencies, the greatest deficits were observed at high spatial frequencies **(Lindberg et al., 1981)**. This study used both an adaptive letter CS test (a method that seeks to find a patient's CS by successively increasing and decreasing contrast of the letter) and the Pelli-Robson CS chart. **Alexander et al. (1992)** found that all RP patients tested exhibited a loss of CS at all letter sizes and luminances tested.

Diabetic Retinopathy (DR): Using sine wave gratings, Hyvärinen et al. found that there was an overall loss of CS in patients who had DR, but CS was especially reduced for low and intermediate spatial frequencies. They showed that CS loss may occur without a corresponding

loss of acuity for patients with background or proliferative DR **(Hyvärinen et al., 2009)**. Khosla et al. found that patients with DR had lower CS compared to controls using the Cambridge low-contrast chart **(Khosla et al., 1991)**. Stavrou et al. found decreased CS for patients with DR compared to controls using the Pelli-Robson CS chart **(Stavrou et al., 2003)**.

Glaucoma: Hawkins et al. found that patients who have glaucoma and relatively good visual acuity had CS losses when tested with the Pelli-Robson CS chart **(Hawkins et al., 2003)**. Using static and temporally modulated sine wave grating patterns, Ross et al. (1984) found that patients with advanced glaucoma experienced CS deficits at all spatial frequencies. Interestingly, the CS losses were primarily found at high spatial frequencies early in the course of the disease, and low frequency CS losses developed in the later stages. **(Ross et al., 1984)**.

Optic Neuritis: Optic Neuritis has been shown to cause selective MC pathway CS deficits and it was proposed that high levels of noise in the visual pathway may, at least in part, account for the CS losses **(Cao et al., 2011)**. Zimmern et al., used sine wave gratings to asses CS losses in patients with optic neuritis. They found that some of the patients experienced CS losses at all spatial frequencies, whereas others had losses only at intermediate and high spatial frequencies **(Zimmern et al., 1979)**. Using the Pelli-Robson CS chart, Trobe et al. found that patients whose acuity returned to normal after the acute phase of ON still exhibited CS deficits six months later **(Trobe et al., 1996)**.

D. Temporal Contrast Sensitivity: In addition to having spatial CS, the visual system also has temporal CS. That is, CS can be measured as a function of duration (or flicker frequency), rather than as a function of spatial frequency (size). For completeness, temporal CS is discussed briefly below, but the focus of the present thesis is on spatial CS (with the exception of Aim 4 in which duration was varied).

The ability of the eye to sum light over time is called temporal summation. Temporal summation has been shown to follow Bloch's Law (Eq. 7) under many conditions:

$$q = L \cdot t^{n}, \qquad (7)$$

where q is a constant value of total luminance energy, n indicates whether summation is complete (n = 1) or partial (0 < n < 1), L is the luminance of the stimulus, and t represents time. This relationship indicates a tradeoff between stimulus luminance and duration **(Gorea, 2015)**. Compared to a stimulus presented briefly at high luminance, q would be similar for a stimulus of lower luminance presented for a longer time.

E. <u>Contrast Measurements in Noise</u>

As discussed above, CS measurement against a uniform background has a long history in vision science, and many different stimulus types have been used over the years. However, it has been proposed relatively recently that adding a measure of CS in visual noise can provide additional information concerning the factors that limit CS **(Pelli et al., 1999)**. The goal of CS in noise measurements is to provide insight into possible mechanisms that limit CS, which cannot be determined based on standard letter CS measurements alone. In part, the logic of noise-based measurements is that the fidelity of all communication, including vision, is inevitably limited by noise. As discussed at length below, CS can be limited by noise arising within the visual pathway, "internal noise," or by a second factor termed "efficiency" **(Pelli et al., 1999, 2004)**.

In noise-based tests, the visual luminance noise that is added to the stimulus is typically made up of random light and dark 'checks' (squares), reminiscent of 'tv snow.' White visual luminance noise can be defined as randomly incremented and decremented luminance that is added to the stimulus. White noise (Fig. 5) has the characteristic that the frequency spectrum has

similar power at all frequencies. Constant power at all frequencies is achieved as long as the noise checks are relatively small **(Kukkonen et al., 1995)**.

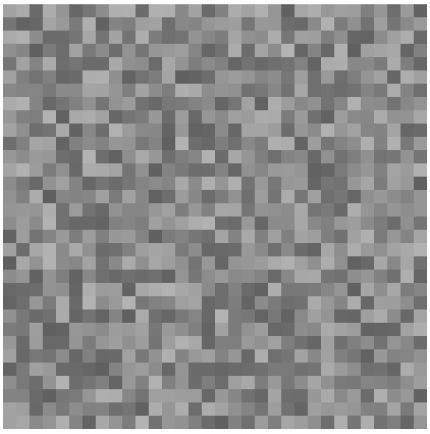

Fig 5, Example of white luminance noise.

If visual performance at threshold is limited by noise, then it follows that the visual system can be considered to have a naturally occurring amount of noise, and determining the amount of this internal noise can be important for understanding the nature of CS losses in patient populations. Noise in the visual pathway can be caused by photon noise, believed to be largely due to the inherent quantum nature of light **(Walls, 1983)**. A second source of internal noise is thought to arise at later sites in the visual pathway ("cortical noise") due to random fluctuations in signal transmission in neuronal networks **(Pelli et al., 1999)**.

Historically, the technique of gradually adding noise to a system until the noise added overtakes the noise naturally present in the system and causes a decrease in the signal to noise ratio (SNR) has been used in the field of engineering for assessing the characteristics of radio receivers and audio amplifiers **(Friis, 1944; Mumford and Schelbe, 1968)**. A similar technique has been used in determining internal noise in the human visual system **(Legge et al., 1987; Pelli 1994)**. To assess the internal noise level in the visual pathway, it is common to add various

amounts of luminance noise, and look for changes in contrast threshold. When the amount of noise added to the visual stimulus is less than the internal noise of the subject, threshold will not be affected. However, when the amount of noise added becomes greater than internal noise, it is expected that threshold will increase.

F. Modeling the Effects of Externally Added Noise on CS

Although many different models of human performance in noise have been used, the most common model is the linear amplifier model (LAM) **(Barlow, 1956)**. The LAM will be used in the present thesis because it is a simple linear model that allows the equivalent noise and efficiency (defined below) to be analyzed.

1. Internal Noise and Efficiency

The LAM assumes that the signal energy at threshold (E_t) is linearly related to the noise spectral density (*NSD*, the power of the noise per unit bandwidth) also known as 'noise power' (N) by the relationship:

$$E_t = k \cdot (N + N_{eq}), \qquad (8)$$

where k represents the slope of the linear function relating signal energy (E_t) and noise power (N), and N_{eq} is the negative of the x-intercept **(Legge et al., 1987 and Pelli and Farell, 1999)**. From Eq. (8), two independent factors that govern CS can be derived: (1) equivalent input noise (N_{eq}), which is an estimate of the noise within the visual pathway and (2) sampling efficiency (reciprocally related to k), which represents the observer's ability to make use of stimulus information relative to an ideal observer (i.e. perfect performance).

2. Measuring CS in Noise in Patient Populations

Internal noise may be higher in patients with ocular disease compared to visually normal individuals. Conversely, efficiency may be lower in patients with ocular disease and higher in

healthy individuals. Determining internal noise and efficiency levels may help explain the source of CS losses in patients. There are a number of studies examining the effect of disease on CS in noise. The following is a brief review.

Amblyopia: Using letters in noise, Pelli et al. found that amblyopes have a decreased efficiency at small letter sizes and abnormally high cortical noise **(Pelli et al, 2004).** Huang et al. found that amblyopes have increased internal noise at all spatial frequencies and an increased impact of external noise at high spatial frequencies **(Huang et al., 2007).** Using Gabor patches in noise**,** Xu et al. also found increased internal noise across all tested spatial frequencies in amblyopic patients **(Xu et al., 2006).** Levi and Klein used sums of sine waves and sine wave noise and found that amblyopes had higher than normal internal noise levels and a loss of CS at high spatial frequencies **(Levi and Klein, 2003).**

Age-related Macular Degeneration (AMD): Using Gabor patches presented in dynamic sine wave noise, Kersten et al. showed decreased CS, decreased efficiency, and higher internal noise for eyes affected with AMD **(Kersten et al., 1988)**.

Retinitis Pigmentosa (RP): Using Gabor patches in noise, McAnany et al. found that patients who have RP had increased internal noise levels compared to normal subjects **(McAnany et al., 2013).** The patients with RP had decreased CS in the absence of external noise, but normal CS in added external noise.

Glaucoma: Yates et al. found that sine wave grating CS deficits increased as the level of external noise increased **(Yates et al., 1998)**.

Optic Neuritis (ON): Flanagan et al. found that using different sized random noise checks, flicker modulation, and chromatic contrast threshold tests, the PC pathway (associated with red/green color sensitivity) was selectively affected in ON **(Flanagan et al., 2005)**. Note

that this is not consistent with the findings of Cao et al., who showed a selective MC pathway CS deficit and a PC pathway contrast gain deficit. The discrepancy between studies may be due to differences in the methods of assessment and that chromatic contrast threshold tests may not selectively target the PC pathway.

G. The Visual Pathway Mediating CS

As discussed above, the visual pathway (MC or PC pathway) mediating letter contrast sensitivity is an important, although not commonly considered, factor in CS measurement. An overview of the visual pathway is illustrated in Fig 6. The transmission of visual information begins in the retina, which contains several types of cells. In the retina, there are approximately 92 million rod cells and 4.6 million cone cells. These two classes of photoreceptors initiate the first stage of vision and provide input into retinal ganglion cells via second order horizontal and bipolar cells **(Curcio et al., 1990)**. Of the 700,000 to 1.5 million retinal ganglion cells the normal human retina **(Watson, 2014)**, approximately 80% are midget ganglion cells that form the beginning of the PC pathway **(Kandel et al., 2000)**. Midget ganglion cells have a slow conduction velocity, red/green color sensitivity **(Schiller & Malepli, 1978; Silveira et al., 2004)**, respond poorly to small changes in contrast, and have small on/off center-surround receptive fields. Approximately 10% of the RGC population consists of parasol RGCs. They were termed 'parasol' cells because of their relatively large cell bodies and dendritic trees. They have a fast conduction velocity, are sensitive to small changes in contrast, but have little to no color sensitivity **(Jacoby et al., 1996)**. Characteristics of the MC and PC pathways are provided in Table 1. In brief, the MC pathway has relatively low spatial resolution **(Derrington & Lennie, 1984)**, high contrast gain, but saturates in response to relatively small contrast increments/decrements **(Shapley, 1990; Pokorny & Smith, 1997; Silveira et al., 2004; Kaplan**

et al., 1990). Although the MC pathway has high temporal resolution (**Pokorny & Smith, 1997; Silveira et al., 2004**) it has little to no color sensitivity **(Schiller & Malepli, 1978; Silveira et al., 2004)**.

	MC	PC
Contrast Sensitivity	High sensitivity, but saturates in response to small contrasts	Lower sensitivity, responds over a broad range of contrasts
Spatial Resolution	Tuned to low spatial frequencies	Tuned to high spatial frequencies
Temporal Resolution	Tuned to high temporal frequencies	Tuned to low temporal frequencies
Color sensitivity	minimal/no	yes

Table 1. Summary of the properties of the MC and PC pathways.

The last 10% of the retinal ganglion cells are tiny bistratified ganglion cells projecting to the koniocellular layers of the LGN, and carry signals from cells with blue/yellow color sensitivity. They are sensitive to medium contrast stimuli, have medium spatial resolution and moderate conduction velocity **(Kandel et al., 2000; Levine, 2000; Kaplan et al., 1990)**. These bistratified cells will not be the focus of this thesis.

The optic nerve fibers composed of retinal axons primarily terminate in the lateral geniculate nucleus (LGN) of the thalamus. The LGN is a multi-layered structure within the thalamus that helps regulate essential functions such as consciousness, sleep, and alertness **(Levine, 2000)**. Layers 1 and 2 of the LGN have large cells, receive projections from the midget RGCs, and are part of the MC pathway. Layers 3 to 6 contain small cells, receive projections from the parasol RGCs, and are part of the parvocellular pathway. From the LGN, visual information is sent on to primary visual cortex and to higher cortical visual centers.

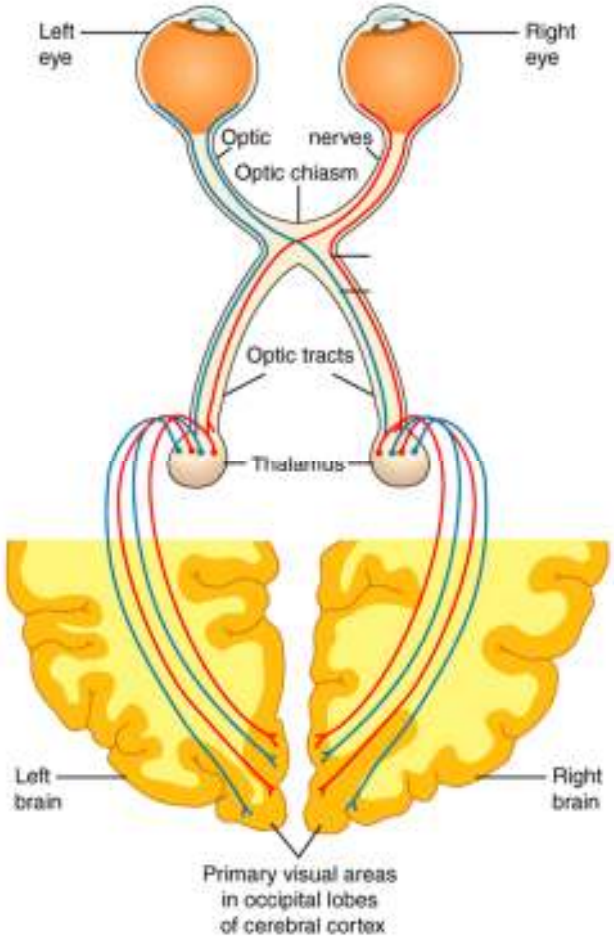

Fig 6, Projections from the retinas of the left and right eyes, through the optic chiasm, along the optic tracts, to the thalamus where the LGN is located. From the thalamus, there are projections to primary visual cortex, then on to higher cortical areas (Wiley, Web). "Human Visual System" is licensed under CC BY 2.0.

H. Using Noise to Target Post-Receptor Visual Pathways

Previous psychophysical work has provided evidence for two independent mechanisms that can mediate visual processing: a slower or 'sustained' mechanism (responses that persist for the duration of the stimulus) and a brief or 'transient' mechanism (responses that occur at the onset and offset of stimulus) **(Mahnilov et al., 2003)**. The terms 'sustained'/'transient' were

originally applied to electrophysiological recordings of the cat retina **(Cleland et al., 1973)**. Subsequently, psychophysicists applied these terms to human-derived thresholds **(Kulikowski et al., 1973)**. These temporal responses may be loosely mapped to the MC and PC pathways, which are known to have similar properties. The 'transient' mechanism is likely analogous to the MC pathway and the 'sustained' mechanism is likely analogous to the PC pathway **(Mahnilov et al., 2003)**.

Mahnilov et al. studied temporal responses ('transient' or 'sustained') in static and dynamic noise for gratings of high and low spatial frequencies **(Mahnilov et al., 2003)**. The static noise paradigm involved presenting a grating target in a constant, unchanging field of noise. The dynamic noise paradigm involved presenting a grating in a constantly changing field of noise, reminiscent of 'tv snow.' Thresholds were measured across a range of stimulus durations to evaluate the temporal properties (sustained/transient) in the two types of noise. The temporal responses in static noise of low and high frequency were found to be transient. Similarly, at low spatial frequencies, the temporal responses were found to be transient in dynamic noise. However, for high spatial frequency stimuli presented in dynamic noise, the temporal responses were sustained **(Mahnilov et al., 2003)**.

McAnany and Alexander used Gabor patches to probe further into the temporal properties associated with static and dynamic noise **(McAnany and Alexander, 2010).** In static noise, they found short temporal integration, whereas in dynamic noise, temporal integration was relatively long. These short and long temporal integration patterns are consistent with Mahnilov's transient and sustained mechanisms **(Mahnilov et al., 2003)**. Furthermore, they found that the CSFs measured in static and dynamic noise are unique: in static noise, the CSF exhibited a low-pass shape, whereas in dynamic noise, the CSF took on a more band-pass shape

(McAnany and Alexander, 2010). Similar results were also found in other work using paradigms that are known to target the MC and PC pathways but are not noise-based **(Leonova, Pokorny, & Smith, 2003)**. Thus, the temporal characteristics of the response and the shape of the CSF depends on the visual pathway mediating CS.

I. Summary

To summarize, CS is a basic task of the visual system and is often measured using letter targets in the clinic. However, the complexities of letter CS, such as the broad range of object frequencies contained in the letters and that two different pathways may mediate letter CS, are not well appreciated. White luminance noise is a tool that may be able to target these two pathways selectively; however, a series of questions regarding the fundamental parameters of a noise-based test must be answered before such a test may be formulated. The overall goal of the present theses is to resolve these questions, develop an optimized noise-based CS test, and then collect proof-of-concept data in the clinic.

III. MAIN METHODS

A. Experimental Design

A series of interrelated Aims were proposed and completed that share common methodologies. Here I will present methods that are shared by multiple Aims. All experiments were approved by an institutional review board at the University of Illinois at Chicago in adherence to the tenets of the Declaration of Helsinki, and all subjects provided written consent before participating.

1. Apparatus

Stimuli were generated using a computer-controlled ViSaGe stimulus generator (Cambridge Research Systems, Kent, UK) and were displayed on a Mitsubishi Diamond Pro (2070) CRT monitor with a 100-Hz refresh rate and a screen resolution of 1024x768. The only source of illumination in the room was the monitor, which was viewed monocularly through a phoropter with the subject's best refractive correction. Luminance values used to generate the stimuli were determined by the ViSaGe linearized look-up table (14-bit DAC resolution) and were verified with a Minolta LS-110 photometer.

2. Letter Contrast

Unfiltered letters were defined by conventional Weber contrast (Eq. 1). However, the contrast of complex images is difficult to define **(Peli, 1990)** and standard definitions such as Weber and Michelson contrast are problematic when applied to complex stimuli. For example, a small high-luminance region (and/or low-luminance region) of a filtered letter would define the contrast value, which could be misleading. To avoid these issues, a relative definition of contrast, which has been used in numerous studies **(McAnany et al., 2008; Hall et al., 2014; Chung et al., 2002; McAnany et al., 2010)**, was used to characterize the filtered letters. Specifically, when the

contrast of the original unfiltered letter was 1.0, the filtered letter was also assigned a relative contrast of 1.0, regardless of the complex luminance distribution of the filtered image.

3. Description of Procedure Used to Measure Threshold

Contrast threshold for letter identification was obtained using a 10-alternative forced-choice staircase procedure. The start of each stimulus presentation was signaled with a brief warning tone. The subject identified the letter verbally, which was then entered by the experimenter; no feedback was given. Only letters from the Sloan set were accepted as valid responses. An initial estimate of threshold was obtained by presenting a letter at a suprathreshold contrast level and then decreasing the contrast by 0.3 log units until an incorrect response was recorded. After this initial search, log contrast threshold was determined using a two-down, one-up decision rule, which provides an estimate of the 76% correct point on a psychometric function **(García-Pérez, 1998)**. Each staircase continued until 16 reversals had occurred, and the geomean of the last 6 reversals was taken as contrast threshold. A reversal is defined as a change in staircase direction (i.e. an increase in contrast following a decrease, or vice versa). Excluding the initial search, the staircase length was typically 35–40 trials, which produced stable measurements. An example is shown below in Fig 7.

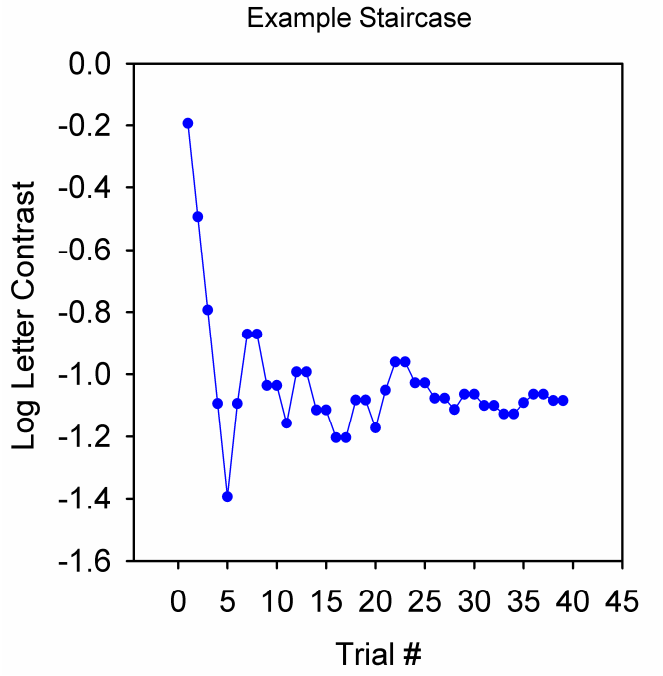

Fig 7, An example staircase in which the contrast of the letter is shown for each trial. An initial search with large steps down in contrast is followed by steps of a decreasing size until a stable contrast value is obtained. Threshold is defined as the geomean of the last 6 reversals.

4. Description of Noise

The root mean square, or RMS, of the noise is defined as follows: x_i is a normalized pixel luminance value (corresponding to a noise check) such that $0 \leq x_i \leq 1$ and $\bar{x}$ is the mean normalized background luminance.

$$RMS = \left[\frac{1}{n-1} \sum_{i=1}^{n} (x_i - \bar{x})^2 \right]^{1/2} \qquad (9)$$

Noise power, or noise spectral density (NSD), is defined as:

$$NSD = RMS^2 \cdot x \cdot y \cdot t \qquad (10)$$

where *x* and *y* are measured in degrees of arc, and *t* in seconds **(Legge, 1987)**. The noise power has units of (deg^2 sec) for dynamic noise, and (deg^2) for static noise. Examples of an unfiltered letter ‘‘D’’ presented in white luminance noise are shown in Fig 8, below.

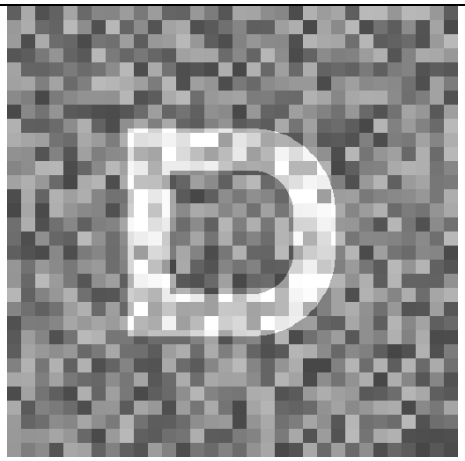

Fig 8, a. Unfiltered D (0.66 contrast) with high 0.25 RMS noise

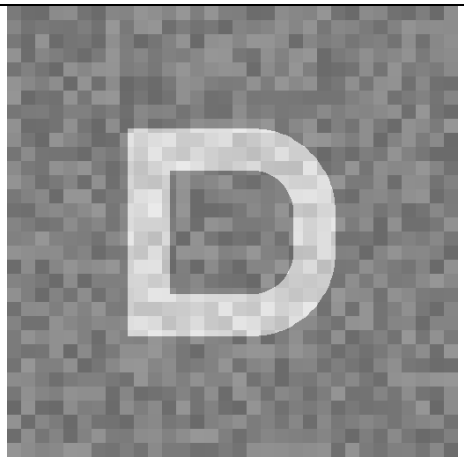

b. Unfiltered D (0.66 contrast) with low 0.10 RMS noise

The mean luminance of the white noise was 50 cd/m^2. The noise fields consisted of independently generated square checks with luminances drawn randomly from a uniform distribution with a RMS contrast of 0.18, except for Aim 2, in which noise power was varied. The noise field covered an area that was about 1.5 times larger than the letter. There were three noise checks per letter stroke (15 noise checks per letter). Unless otherwise specified, the noise temporal presentation was “asynchronous,” such that the onset of the noise preceded the onset of the letter by 100 ms and the offset of the noise followed the offset of the stimulus by 100 ms. This temporal arrangement is commonly used in noise-based studies **(McAnany & Alexander, 2009; McAnany and Alexander, 2010; McAnany et al., 2013)**.

B. Analysis

1. Description of Object Frequency Measurement

Spatial low- and high-pass filtering was employed to derive the object frequencies mediating letter identification. Letters from the Sloan set were spatially high- or low-pass filtered with a set of two-dimensional Gaussian filters. The object frequency cutoffs of the filters ranged from 0.9 to 21.0 cpl in 10 steps spaced approximately 0.15 log units apart, and the filter was applied by convolution with the letter in the frequency domain (see appendix for the MATLAB code used for the letter filtering). Examples of unfiltered, low-pass filtered, and high-pass filtered letters that were 66% contrast are shown in Fig. 9.

Fig 9, a. Unfiltered H, 0.66 contrast

b. LP Filtered H, 5.63 cpl cut off, 0.66 contrast

c. HP Filtered H, 5.63 cpl cutoff, 0.66 contrast

Contrast threshold was measured for various filter cutoffs (0.94, 1.32, 1.87, 2.64, 3.75, 5.28, 7.50, 10.51, 15.00, and 21.00 cpl) for the low- and high-pass filters. Contrast threshold was plotted as a function of letter cutoff and the data were fit piecewise with two linear functions using a least-squares criterion: one region was constrained to have a slope of 0, and the slope of the second region was unconstrained. The high-pass and low-pass functions in each plot were fit separately and are represented by the solid lines in (Figure 10, below).

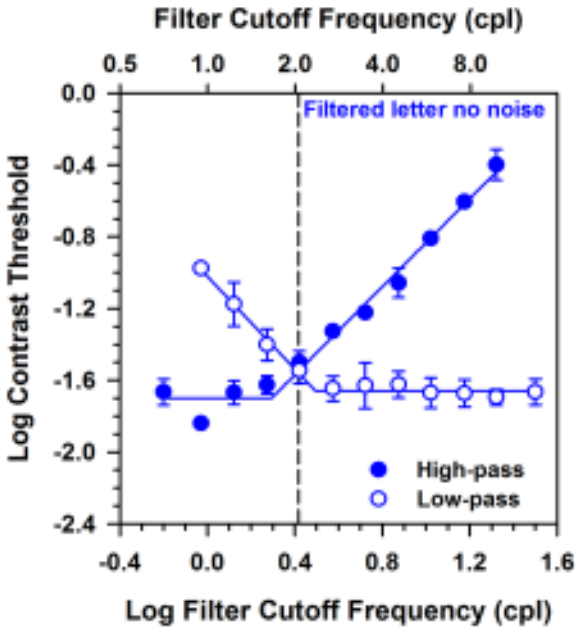

Fig 10, Example function showing log contrast threshold for high- and low-pass filtered letters. The two part linear fits for both low- and high-pass functions are shown, and the point at which they cross is noted with a dotted vertical line.

There is a region over which threshold is independent of the filter cutoff and a second region over which log contrast threshold increased or decreased linearly with the filter cutoff. The logic is that if frequencies that are not being used to identify a letter are removed, threshold will not increase (horizontal regions of zero slope in Fig. 10). However, if the frequencies used in letter identification are removed, threshold will increase (regions of unit slope in Fig. 10).

The cutoff object frequency at which the functions crossed (indicated by the vertical dashed lines in Fig. 10) was taken as an index of the center of the band of object frequencies mediating letter identification. This point, which was also used in previous reports **(Alexander & McAnany, 2010; McAnany & Alexander, 2008)**, represents approximately equal elevations of log contrast threshold, compared to the threshold values obtained with minimally filtered letters.

IV. SPECIFIC AIM 1: IDENTIFY THE OPTIMAL SET OF LETTERS FOR USE IN LETTER CONTRAST SENSITIVITY TESTING

A. Introduction

Letters are commonly used in the clinical assessment of visual function (e.g., the Lighthouse Distance Visual Acuity Chart and the Pelli-Robson CS chart). The 10 letters from the Sloan set are particularly useful for CS testing because these letters set have been shown to be similarly identifiable when presented at a large size (1.3 log MAR [logarithm of the minimum angle of resolution]) **(Alexander et al., 1997)**. The use of a set of similarly identifiable letters is important to ensure that the differences within a line of letters on a CS chart (inter-letter differences) are less than the difference between lines. However, inter-letter differences in CS become greater (differences of about a factor of 2 among the 10 letters) for letter sizes that approach the visual acuity limit **(Alexander et al., 1997)**. The explanation for the increased inter-letter CS differences at small sizes may be related to the object frequency information **(Parish et al., 1991)** that mediates letter CS for small versus large letters. That is, identification of small letters tends to be based on low object frequencies that correspond to the general shape of the letter **(Alexander et al., 1997; Anderson et al., 1999; Bondarko et al., 1997; Majaj, 2002)**, whereas higher object frequencies that correspond to edges are used for larger letters **(Alexander et al., 1997; Majaj, 2002; McAnany et al., 2008)**. This suggests that inter-letter differences may vary for different letter sizes, and indeed, at smaller sizes the differences tend to become greater **(Alexander et al., 1997)**.

Previous studies comparing inter-letter CS differences have only been performed under conditions in which the letters were presented against a uniform field. As such, the magnitude of inter-letter differences in luminance noise is unknown and it is possible that inter-letter threshold

differences are larger in noise. For example, noise masking of the gap in the letter ‘‘C’’ may markedly elevate threshold, compared with a smaller threshold elevation due to noise masking of other Sloan letters that contain redundant information. Additionally, there is evidence from the literature that luminance noise can shift the object frequency information mediating letter CS to higher values **(Oruc and Landy, 2009).** This would be expected to reduce inter-letter threshold differences, as high object frequencies convey letter identity information that is more reliable than low object frequencies. At present, the effect of luminance noise on inter-letter CS differences is not well understood. Consequently, the purpose of this Aim is to determine the inter-letter CS differences for letters presented with and without added luminance noise. The results of this Aim formed the basis for an article published in 2015 **(Hall et al., 2015)**.

B. Methods

1. Subjects

The author (age 25 years) and two other subjects (22 and 34 years) with no history of eye disease, normal best-corrected visual acuity assessed with the ETDRS (Early Treatment of Diabetic Retinopathy Study) distance visual acuity chart **(Ferris et al., 1982)**, and normal CS assessed with the Pelli-Robson CS chart served as subjects.

2. Apparatus and Procedure

The apparatus and stimuli are described in the Main Methods section. Contrast threshold for letter identification was measured using letters from the Sloan set. The letter size was equivalent to 1.5 log MAR (the letter size used for the Pelli-Robson CS chart). Letters from the standard Sloan set were presented for an unlimited duration against a uniform adapting field (50 cd/m^2) or in additive white noise that consisted of independently generated square checks with luminances drawn randomly from a uniform distribution with a RMS contrast of 0.18. The onset

and offset of the noise and stimulus were identical (i.e., synchronous static noise). The CS measurement procedures are described in the Main Methods section, except that there were ten interleaved staircases, one for each letter, which allowed us to assess the extent to which the individual letters have similar contrast thresholds. For each 1-hour testing session, a noise paradigm (noise present or absent) was selected pseudorandomly for testing.

3. Analysis

Inter-letter contrast threshold differences were predicted based on a previous approach of quantifying the ‘‘dissimilarity’’ among letters **(Anderson and Thibos, 2004)**. In brief, the 10 letters within the set were summed to create a complex hybrid image. Then, each individual letter was subtracted from the mean image and the RMS contrast of the difference image for each individual letter was calculated. Equation 9 was used to derive the RMS contrast of the difference image, as described in the Main Methods section, but x_i here refers to a normalized pixel value in the difference image (rather than the normalized noise check luminance). Individual letters that are highly distinct from the other letters in the set have high RMS contrast values. Of note, dissimilarity can equivalently be calculated in the frequency domain by obtaining the frequency spectrum of the difference image, as described elsewhere **(Anderson and Thibos, 2004)**.

C. Results

Fig. 11 plots the mean log CT for the three visually normal subjects for each letter of the Sloan set, in the presence (blue) and absence (red) of luminance noise. The solid lines show the model predictions, and the error bars show ± 1 SEM of the subjects. The model predicts that threshold will be highest for letters D, R, and S, indicating that these letters are most similar to

the mean of all letters, whereas letter V has the lowest expected threshold, indicating that V is the least like the other letters.

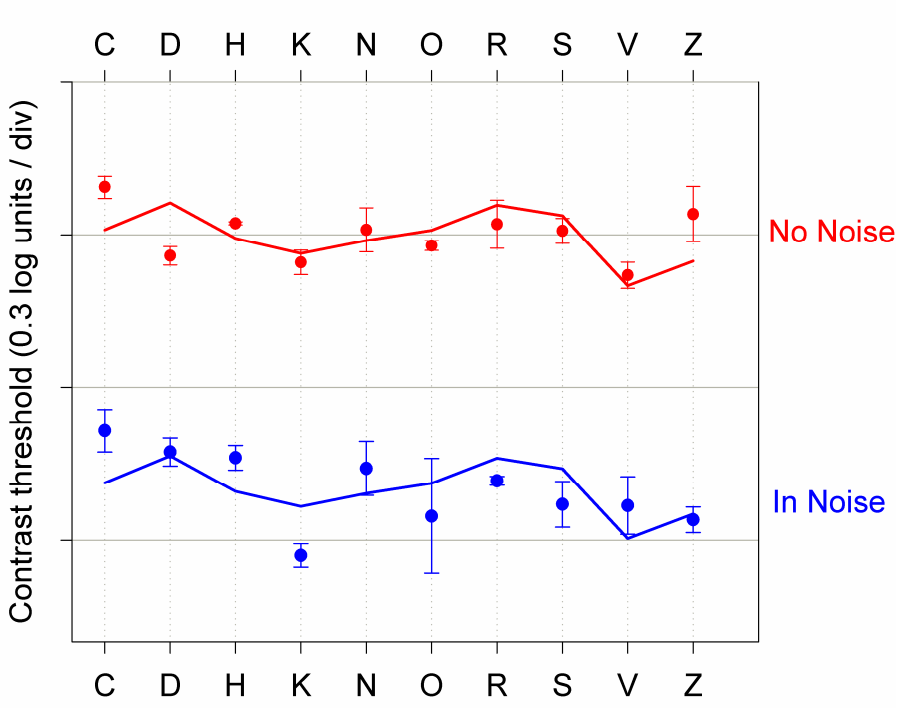

Fig 11, Contrast threshold for the three visually normal subjects for Sloan letters presented without (red) and with (blue) visual luminance noise. The solid lines represent the predicted contrast threshold for the letters without noise and in noise, respectively, based on the difference model. The error bars show ± 1 SEM of the subjects.

The pattern of mean CT obtained from the three subjects generally followed the model predictions. The predictions matched the mean data for measurements made in the absence of noise (mean squared error between the data and model = 0.003) and in noise (mean squared error between the data and model = 0.004) similarly. The largest differences from the predicted CT were observed for the letters K and O for measurements made in noise (blue). The no noise condition (red) had noticeable deviations from the model prediction for letters C, D and Z.

In general, the results indicate that the inter-letter difference in contrast threshold was approximately 1.5 when presented against a uniform field (without noise) and was somewhat larger when presented in noise (the inter-letter differences increased slightly to a factor of about 1.8). Additionally, the removal of the letters C and V from the Sloan letter set would be expected to reduce the inter-letter contrast threshold difference from about 0.17 log units (full Sloan set) to 0.09 (eight letters).

D. Discussion

The goal of the present Aim was to determine the extent to which individual Sloan letters have similar contrast thresholds for letters in the presence and absence of white luminance noise. The individual differences among letters were generally predicted by their similarity or difference compared to the mean of the letter set. The model predicted that letters like 'D', 'R', and 'S' would have higher thresholds, as these three letters are similar to the to the mean of the letter set. Additionally, the letters O and C are frequently confused, which may have contributed to the relatively high threshold for the C, if subjects tended to guess O more frequently than C. The letter V is somewhat unique, consisting of two diagonal components. This letter was most different from the mean of the letter set and the human threshold measurements were relatively low for this letter.

These data will be of use in the development of our optimized noise test. For the optimized test, the full Sloan set (10 letters) will be used because the minor improvement in inter-letter threshold differences is largely offset by the increased likelihood of correct guessing that would be expected for a smaller set of letters. The letter in noise test can also be developed with confidence that the addition of noise does not substantially elevate the inter-letter threshold differences.

V. SPECIFIC AIM 2: DETERMINE THE EXTENT TO WHICH THE SPATIAL AND TEMPORAL CHARACTERISTICS OF LUMINANCE NOISE CAN BE MANIPULATED TO TARGET THE MC AND PC PATHWAYS.

A. Introduction

Many studies have compared CS in the presence and absence of luminance noise **(e.g. Parish and Sperling, 1991; Majaj et al., 2002; Manahilov et al., 2003; McAnany et al., 2010)**. However, CS can be mediated by two post receptor pathways, the MC and PC pathways, and it is not clear if noise affects the pathway mediating CS. Previous work suggests that dynamic and static noise may target sustained- and transient-like mechanisms, respectively **(Manahilov et al., 2003)**. The sustained-like mechanism is likely to be related to PC pathway function, whereas the transient-like mechanism is likely to be related to the MC pathway. However, CS in static and dynamic noise has not been compared directly to CS measured under conditions known to target the MC and PC pathways. Thus, the extent to which static noise targets the MC pathway and dynamic noise targets the PC pathway is presently uncertain.

In this Aim, the extent to which the spatial and temporal characteristics of luminance noise can be manipulated to target the MC and PC pathways will be determined. To do this, thresholds for high- and low-pass filtered letters will be measured in static and dynamic noise, which will permit the object frequency mediating CS to be determined in these two noise types. The object frequencies measured in static and dynamic noise will be compared to those measured under paradigms known to target the MC and PC pathways: the "steady-pedestal paradigm" and the "pulsed-pedestal paradigm" **(Leonova et al., 2003).** Of note, it is difficult to infer the pathway mediating CS from measures of CS alone, as these depend strongly on factors such as

noise power and stimulus duration. Object frequency is less dependent on these factors and therefore provides a better index of the visual pathway mediating CS. Object frequency will be used throughout this thesis as an index of the pathway mediating CS.

B. Methods

1. Subjects

The author (aged 27), one experienced subject (36 years), and one naïve subject (27 years) who have no history of eye disease, normal best-corrected visual acuity assessed with the ETDRS distance visual acuity chart, and normal CS assessed with the Pelli-Robson CS chart served as subjects.

2. Apparatus and Procedure

The apparatus and stimuli are described in the Main Methods section. Letter size for this Aim was equivalent to 1.8 log MAR (similar to the letter size used for the Pelli-Robson CS chart). For the static and dynamic noise paradigms, letters were presented for a 50 ms duration against either a static (unchanging) or dynamic (changing every 10 ms) additive white luminance noise field that had a mean luminance of 50 cd/m^2. A range of RMS values was used in static and dynamic noise (RMS = 0.023, 0.034, 0.045, 0.068, 0.090, 0.135, 0.180, 0.270).

Under the steady-pedestal paradigm, which was used to target the MC pathway, a letter target was presented against a steady adapting field (Fig. 12, top). This creates only a small, brief change in contrast during stimulus presentation, which the MC pathway is sensitive to. Under the pulsed-pedestal paradigm, which is used to target the PC pathway, a letter target and luminance pedestal were presented simultaneously (Fig. 12, bottom), which creates a large, brief change in contrast, saturating the sensitive MC pathway and causing the PC pathway to mediate CS.

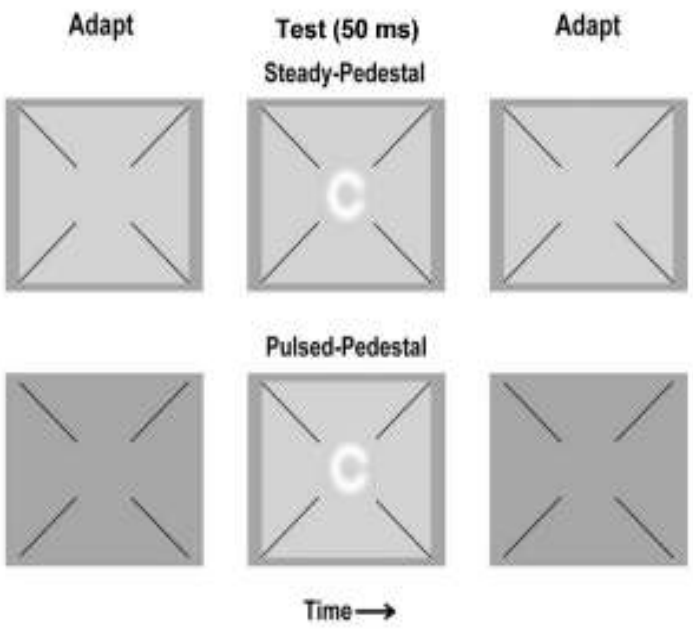

Fig 12, Steady- and pulsed-pedestal paradigms. Under the steady-pedestal paradigm (top), the subject adapted to a luminance pedestal and a letter was briefly presented (50 ms). Under the pulsed-pedestal paradigm (bottom), the subject adapted to a low luminance field and the luminance pedestal and letter were presented simultaneously (50 ms).

For each 1-hour testing session, a static or dynamic noise paradigm (and therefore one noise RMS value) was selected pseudorandomly for testing. For the static paradigm, one subject (the author) obtained data at all RMS values over a total of 9 sessions. For the dynamic noise paradigm, all three subjects completed 9 sessions to measure object frequency at each of the 9 RMS values. For the steady- and pulsed-pedestal paradigms, the three subjects completed 1 session for each paradigms.

3. Analysis

The object frequency mediating letter CS was determined for each RMS by high- and low-pass filtering in either static or dynamic noise using the methods described in the Main Methods section, and similarly for the steady- and pulsed-pedestal paradigms.

C. Results

Fig. 13 shows log object frequency plotted versus log noise power for measurements made in dynamic (green circles) and static (red diamonds) noise. The blue and black lines denote the PC and MC object frequency values measured under the pulsed- and steady-pedestal paradigms, respectively. The mean pulsed-pedestal object frequency value was approximately 0.80 log cpl and the steady-pedestal value was approximately 0.42 log cpl. In static noise, object frequency was approximately 0.44 log cpl, regardless of the noise power. The static noise data fall along the predicted MC line obtained under the steady-pedestal paradigm. The data for static noise were fit with a horizontal line (zero slope). In dynamic noise, the object frequency data fall along the predicted MC line only for low noise powers. With increasing dynamic noise RMS, the center frequency increased systematically, reaching a plateau near the PC value obtained from the pulsed-pedestal paradigm. The data for the dynamic noise condition were fit with a sigmoidal (Weibull) function. The use of a Weibull function is arbitrary to the extent that any sigmoidal function would likely have been appropriate to describe the shift from MC pathway processing to PC pathway processing.

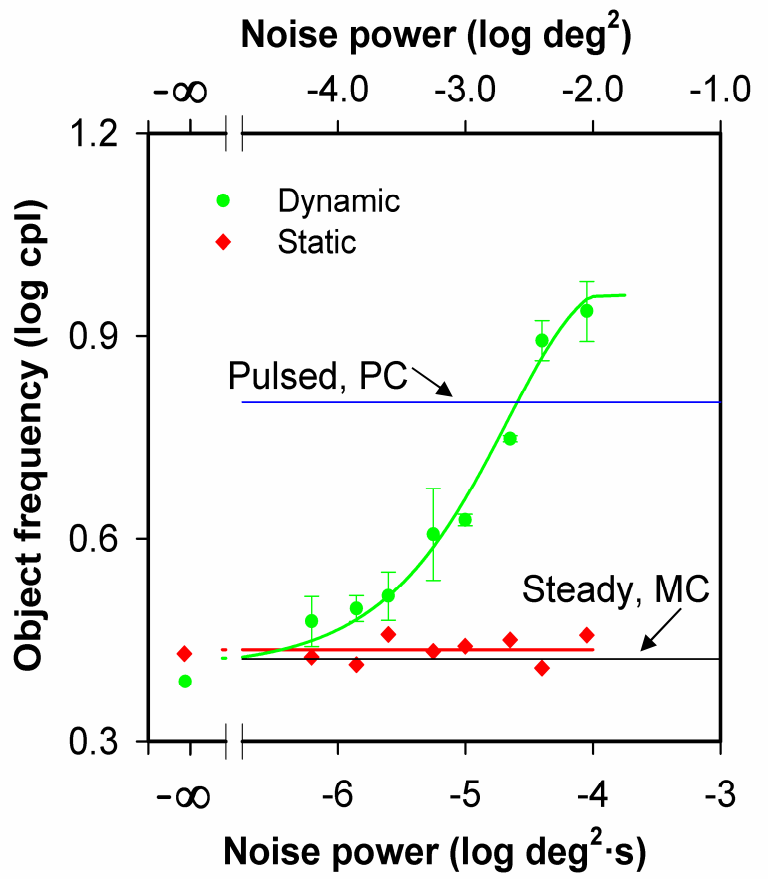

Fig 13, Mean (± SEM) log object frequencies used in static (red) and dynamic (green) noise tested over a range of noise powers for one (static) and three (dynamic) visually normal subjects. The object frequencies for the dynamic data transition from low object frequencies at low noise powers, to higher object frequencies at high noise powers. For all noise powers, the object frequency mediating CS in static noise remains constant. The mean data from the steady-pedestal and pulsed-pedestal paradigms were fit with functions as described in the text (red and blue lines respectively).

D. Discussion

The similarities in object frequency obtained under the static noise and steady-pedestal paradigm (approximately 2 cpl) for all noise power values suggest that the MC pathway mediates performance in static noise. Conversely, the similarities in object frequency obtained under the pulsed-pedestal and dynamic noise paradigms at high noise levels (approximately 8 cpl) suggests that the PC pathway mediates performance in dynamic noise of high RMS. It was found that a noise power greater than -5.5 log deg^2 s was necessary to begin increasing the object frequency beyond the expected MC pathway range. The noise power -5.5 log deg^2 s is significant because this is approximately the level of noise naturally present in the visual system (discussed further in Aim 5). For noise power greater than -5.5 log deg^2 s, the luminance noise added to the stimulus dominates and threshold is dependent on this added noise value. From approximately -5.5 to -4.0 log deg^2 s, the object frequency mediating CS falls between the expected MC and PC pathway values, suggesting that there may be some shared MC and PC processing across this range. Regardless, for the purposes of developing the optimized noise-based CS test, the results of Aim 2 indicate that, at least for the duration and letter size used herein, the MC pathway can be targeted by using static noise of any noise power, whereas the PC pathway can be targeted using dynamic noise of high noise power.

VI. SPECIFIC AIM 3: DETERMINE THE EFFECT OF LETTER SIZE ON THE OBJECT FREQUENCY USED FOR LETTER IDENTIFICATION UNDER THE STEADY/PULSED AND STATIC/DYNAMIC NOISE PARADIGMS

A. Introduction

It has been shown that the object frequency used to identify letters changes with letter size **(Majaj et al., 2002; Chung et al., 2002)**. Using band-pass filtered letters, Chung et al. found that the log object frequency mediating letter identification increased linearly as log letter size increased with a slope of 1/3 **(Chung et al., 2002).** Similarly, Majaj et al. found a linear relationship with a slope of 1/3 between log object frequency and log letter stroke frequency (size). The work described in Aim 2 used letters of a constant large size (1.8 log MAR, which is somewhat larger than the letter size used for the Pelli-Robson chart when viewed from 1 m). The current implementation of the Pelli-Robson chart uses letters that subtend 1.5 log MAR, but early versions of the Pelli-Robson chart specified a 3 m test distance and letters that subtended 0.8 log MAR **(Pelli et al., 1988)**. It is possible that CS may be differently affected by ocular disease at these different letters sizes and the use of both may have advantages. Along these lines, other chart-based tests of letter CS have been proposed that use letters that are smaller than the current 1.5 log MAR standard. Based on the findings of Majaj and Chung, changing the letter size would affect the object frequency used to identify the letters. As such, different information may be used to identify letters in these tests of CS, but the effect of letter size on the information used to identify letters is not generally considered in clinical tests of letter CS.

Therefore, it is important to understand how letter size impacts the object frequency used to identify letters and, for our purposes, to determine if the MC and PC pathways can be targeted

selectively at different letter sizes. In Aim 3, we will determine whether or not the static and dynamic noise paradigms effectively target the MC and PC pathways for a range of letter size. As in Aim 2, measurements will be performed under the steady- and pulsed-pedestal paradigms that have been shown to target the MC and PC pathways and these measurements will be compared to those obtained under the static and dynamic noise paradigms.

B. Methods

1. Subjects

Three visually normal subjects, the author (age 27) and two naïve observers (25 and 27 years), were tested in this Aim. The subjects have no history of eye disease, normal best-corrected visual acuity assessed with the ETDRS distance visual acuity chart, and normal CS assessed with the Pelli-Robson CS chart.

2. Apparatus and Procedure

The apparatus and stimuli are described in the Main Methods section. Contrast threshold for letter identification was measured using letters from the Sloan set. The letter sizes were equivalent to 1.0, 1.2, 1.4, 1.6 and 1.8 log MAR. Letters were presented for 50 ms in either static or dynamic additive white luminance noise, or under the steady- and pulsed-pedestal paradigms (described in Aim 2). Contrast threshold for all paradigms was determined using a 10-alternative forced-choice staircase procedure. The object frequency mediating letter CS was determined for each letter size in static noise, dynamic noise, and under the steady- and pulsed-pedestal paradigms by high- and low-pass filtering, as described in the Main Methods section. For each 1-hour testing session, a paradigm and letter size were selected pseudorandomly for testing. Each subject participated in 20 individual test sessions, each lasting approximately 1 hour.

3. Analysis

In Aim 3, object frequency was measured for different letter sizes, allowing for plots of log object frequency versus log letter size (log MAR) to be generated. Eq. 11, from **Alexander and McAnany (2010)** was used to fit the plots of log object frequency F_o versus letter size. In the equation below, F_{omin} is the asymptotic object frequency at small letter sizes and MAR_{crit} is the value of MAR where F_o is twice F_{omin}. F_{omin} and MAR_{crit} control the vertical and horizontal scaling of the function.

$$F_o = F_{o_{\min}}(1 + (MAR_{crit} / MAR)) \quad (11)$$

C. Results

Fig 14 shows the mean log object frequency ± SEM of the three subjects plotted versus letter size (log MAR). The four lines represent the fit of the data for the three subjects based on Eq. 11, for each of the four paradigms. The log object frequency mediating CS for all paradigms tended to increase as letter size was increased. Under the static noise (red diamonds) and steady-pedestal (gray triangles) paradigms, log object frequency increased slightly, but systematically, as letter size increased. In comparison, log object frequency increased sharply under both the dynamic noise (green circles) and pulsed-pedestal paradigms (blue squares).

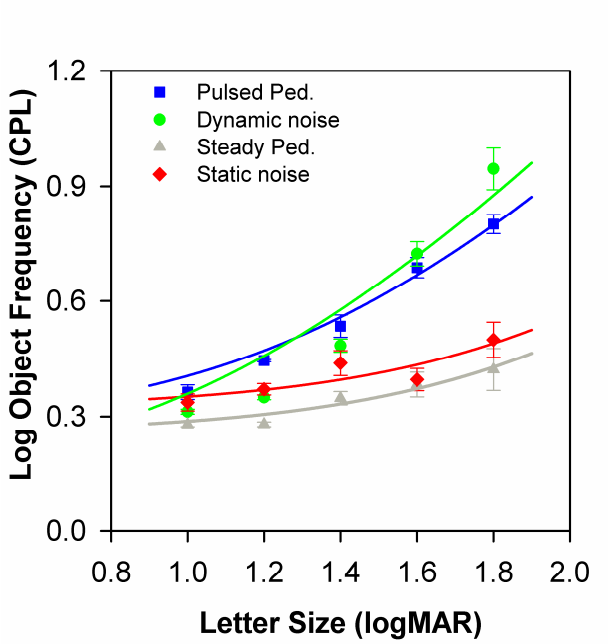

Fig 14, Mean (±) SEM log object frequency at 5 letter sizes for the steady-pedestal (gray), static noise (red), dynamic noise (green), and pulsed-pedestal (blue) paradigms as a function of letter size for three visually normal subjects. Lines represent the fits of the data as described in the text.

In order to compare the object frequencies measured under the four paradigms at the five letter sizes, a two-way repeated measures ANOVA was performed. The ANOVA indicated statistically significant effects of paradigm [$F(6,24) = 81.30$, $p < 0.001$] and size [$F(4,24) = 73.507$, $p < 0.001$]. ANOVA also indicated a significant interaction between paradigm and size [$F(12,24)=20.22$, $p < 0.001$], indicating that the differences among the four paradigms depended on size. Follow-up comparisons are shown below in Table 2. Results indicated that the object frequency values obtained under the steady-pedestal and static noise paradigms were not significantly different (on average, the object frequencies differed by only 0.01 log units). Follow-up comparisons also indicated that the object frequency values obtained under the

pulsed-pedestal and dynamic noise paradigms were not significantly different (on average, the object frequencies differed by only 0.06 log units).

Comparison	Diff of Means	t	P	P<0.050
Dynamic vs. Pulsed	0.059	3.228	0.108	No
Static vs. Steady	0.009	0.482	1.000	No
Dynamic vs. Steady	0.233	12.654	<0.001	Yes
Dynamic vs. Static	0.224	12.172	<0.001	Yes
Pulsed vs. Steady	0.173	9.426	<0.001	Yes
Pulsed vs. Static	0.165	8.945	<0.001	Yes

Table 2. Pairwise Multiple Comparisons.

D. Discussion

The goal of the present Aim was to determine the ability of the static and dynamic noise paradigms to target the MC and PC pathways over a range of letter sizes. The results for the static and dynamic noise paradigms were compared to those obtained under the steady- and pulsed-pedestal paradigms, as there is evidence that these paradigms selectively target the MC and PC pathways **(Pokorny & Smith, 1997)**. The results of this Aim indicate that is possible to target the MC and PC pathway effectively with static and dynamic noise, respectively, for large letters (1.4 log MAR or larger). However, similar object frequencies mediated letter identification for small letters. As such, it is difficult to determine which pathway mediates performance for small letters. An inability to clearly separate the MC and PC pathways for small targets (high spatial frequencies) was also reported by Leonova et al. who showed that CS for the steady- and pulsed-paradigms is similar at high spatial frequencies (small sizes). Leonova et al. speculated that this may be because the MC pathway has poor sensitivity for high spatial frequencies, so the PC pathway likely mediates CS at high spatial frequencies irrespective of the

paradigm **(Leonova et al., 2003)**. Based on these results, we conclude that large letter sizes (1.4 log MAR or larger) are most effective for targeting the MC and PC pathways selectively in static and dynamic noise A letter size of 1.8 log MAR will be used in the paradigm developed for clinical testing.

VII. SPECIFIC AIM 4: EVALUATE THE ABILITY OF STATIC AND DYNAMIC NOISE TO TARGET THE MC AND PC PATHWAYS ACROSS A SERIES OF LETTER EXPOSURE DURATIONS

A. Introduction

The steady- and pulsed-pedestal paradigms effectively target the MC and PC pathways for brief stimulus durations, like those used in Aims 2 and 3 **(Pokorny & Smith, 1997)**. However, for durations longer than approximately 50 ms, the ability to target the MC and PC pathways selectively using these two paradigms is questionable. As the stimulus duration is increased, the pulsed-pedestal paradigm becomes more like the steady-pedestal paradigm (e.g. very long pulses can be considered as a "steady" presentation). This is consistent with observations that the MC pathway has a temporal integration period of approximately 50 ms, whereas the temporal integration of the PC pathway approximately 200 ms **(Pokorny, 2011)**. However, short stimulus durations may not be suitable for patient populations who have large functional deficits for briefly presented stimuli. CT for these patients can be elevated beyond the range that can be measured with our instrumentation. By increasing the duration of the stimulus, patient sensitivity may be increased (CT reduced) into the range that can be measured.

In Aim 4, the effect of stimulus presentation duration on our ability to target the MC and PC pathways will be determined. Object frequencies will be measured for letter durations ranging from 50 to 400 ms in static and dynamic noise, and compared to results obtained under the steady- and pulsed-pedestal paradigms.

B. Methods

1. Subjects

The author (aged 27 years), an experienced psychophysical subject (36 years), and a naïve subject (27 years) who have no history of eye disease, normal best-corrected visual acuity assessed with the ETDRS distance visual acuity chart, and normal CS assessed with the Pelli-Robson CS chart served as subjects.

2. Apparatus and Procedure

The apparatus and stimuli are described in the Main Methods section. Contrast threshold for letter identification was measured using letters from the Sloan set. The letter size was equivalent to 1.8 log MAR (similar to the letter size used for the Pelli-Robson CS chart). Letters were presented for 50, 100, 200, and 400 ms in either static or dynamic additive white luminance noise that had an RMS value of 0.18. Additionally, measurements were made under the steady- and pulsed-pedestal paradigms **(Leonova et al., 2003)** in the same subjects at the same durations. The object frequency mediating letter CS was determined by high- and low-pass filtering for each stimulus duration in static and dynamic noise, as well as for the steady- and pulsed-pedestal paradigms with the procedure described in the Main Methods section.

For each 1-hour testing session, a paradigm (static/dynamic/steady/pulsed) and one stimulus duration was selected pseudorandomly for testing. Each subject underwent 16 individual testing sessions that were each approximately one hour in duration.

C. Results

In Figure 15, the mean log object frequency for the three subjects is plotted as a function of log target duration for data obtained under the steady (gray triangles), pulsed (blue squares), static (red diamonds) and dynamic (green circles) paradigms (error bars represent ±SEM). The

figure shows that for the steady- and pulsed-pedestal-paradigms, the object frequency mediating CS differed at short durations (e.g. 0.47 log cpl and 0.77 log cpl under the steady- and pulsed-pedestal paradigms, respectively, at 50 ms). However, as the duration was increased, the object frequency decreased under the pulsed-pedestal paradigm and increased under the steady-pedestal paradigm. These data were fit with linear regression lines that predicted that the object frequency measured under the two paradigms would be equal at approximately 770 ms. In contrast to these results, the object frequency mediating CS was generally independent of duration in static (0.51 log cpl) and dynamic (0.80 log cpl) noise. The static (red diamonds) and dynamic (green circles) data were also fit with linear regression lines, but the slopes of these fits were not significantly different from zero (both $t < 2.18$, $p > 0.16$). As such, these data were fit with straight lines of zero slope.

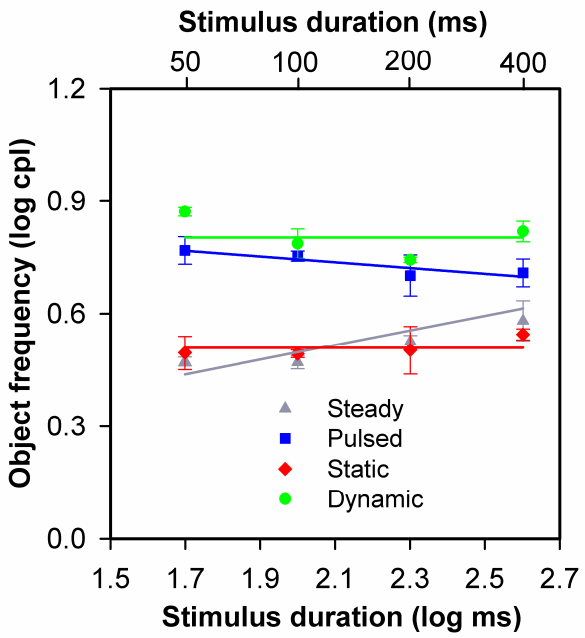

Fig 15, Log object frequency as a function of log target duration measured under the steady-pedestal (gray), static noise (red), pulsed-pedestal (blue), and dynamic noise (green) paradigms for three visually normal subjects. Error bars are ±1 SEM.

D. Discussion

The goal of the present Aim was to determine the ability of the static and dynamic noise paradigms to target the MC and PC pathways at different durations. The results obtained under the noise paradigms were compared to those obtained under the steady- and pulsed-pedestal paradigms, which are known to target the MC and PC pathways at short durations **(Leonova et al., 2003)**. The static and dynamic noise paradigms appear to target the MC and PC pathways across a broad range of stimulus durations. In contrast, the steady- and pulsed-pedestal paradigms' ability to target the MC and PC pathway deteriorated at longer durations, as expected form previous work **(Pokorny & Smith, 1997)**. Because the static and dynamic paradigms were able to effectively target the MC and PC pathways over the entire 50-400 ms range of stimulus duration, we propose to use a stimulus duration of 200 ms for implementation in the clinical paradigm that will be applied in Aim 5. We anticipate that 200 ms is long enough to permit sensitivity measurements in patients with substantial CS losses, but short enough to prevent voluntary eye movements **(Purves et al., 2001)**.

VIII. SPECIFIC AIM 5: MEASURE MC AND PC PATHWAY LETTER CS IN PATIENTS WITH OPTIC NEURITIS

A. Introduction

The foundation for an optimized noise-based CS test was developed in Aims 1-4. The optimized parameters obtained from these Aims will be used to develop a noise-based letter CS test that can target selectively the MC and PC pathways. This test will be applied in Aim 5 to a small sample of patients who have optic nerve disease to provide proof of concept for its use in a patient population.

Optic Neuritis (ON): ON is characterized by inflammation and demyelination of the optic nerve. Two-thirds of ON cases occur in women and the condition typically affects those who are between 20 and 50 years old at a rate of about 3 per 100,000 people in the US **(Frohman, 2005)**. ON is highly associated with multiple sclerosis (MS), occurring in 50% patients with MS at some time during the course of their illness **(Balcer, 2006)**. Other common immune conditions that are associated with ON include Lupus, syphilis, sarcoidosis, Lyme disease, and West Nile virus.

ON most often manifests monocularly, but in rare cases (10% of patients) it occurs binocularly **(De la Cruz, 2006)**. An autoimmune reaction, initiated by an underlying autoimmune condition, causes inflammation of the optic nerve sheath, which in turn, typically results in optic nerve edema and demyelination **(Pau, 2011).** Note, however, that ON does not cause demyelination in call cases **(Behbehani, 2007)**. The inflammation of the optic nerve is thought to underlie the commonly reported monocular pain that is exacerbated by eye movement, and visual acuity loss. The onset of these symptoms typically develops rapidly (over hours or

days) **(Foroozan, 2002; Balcer, 2006)**. The characteristic rapid onset is helpful in the diagnosis of ON, particularly for patients who have known autoimmune disorders.

In addition to the rapid onset of ocular pain, a number of functional tests can be helpful in the diagnosis of ON and for describing the visual dysfunction in these individuals. Visual acuity is reduced in approximately 90% of patients and color perception is frequently altered (dyschromatopsia) **Foroozan, 2002; Balcer, 2006**. Visual field perimetry is almost always performed in these patients, as this test has been shown to be useful in monitoring the recurrence or progression of ON **(Kedar, 2011)**. Most commonly, perimetry is performed with the Humphrey visual field (HVF) analyzer. In brief, the HFV analyzer maps sensitivity throughout the visual field (typically 24 or 30 degrees) by presenting stimuli of varying intensity at pre-defined visual field locations and requiring the patient to press a button when the stimulus is detected. In patients with ON, the HVF defect is typically characterized by a central scotoma, consistent with their acuity and color vision defects. Less commonly, diffuse field loss, altitudinal, arcuate, and hemianopic, defects occur.

The clinical course of ON is characterized by acute ocular abnormalities, as described above, and chronic visual abnormalities that are typically more subtle. Ninety percent of patients recover from the acute symptoms of visual field loss within six months, and most patients recover visual acuity within one year. However, chronic symptoms following the acute phase that consist of CS loss, color vision abnormalities, and stereo acuity deficits can persist for years, especially for patients who have MS **(Trobe, 1996; Brusa, 2001)**.

Although CS loss is commonly observed in these patients, which is consistent with their HVF abnormalities, the nature and extent of the CS deficit is not well understood. It is possible

that one post-receptor pathway undergoes damage or has a greater deficit. In fact, previous work has shown that there is a selective MC pathway CS deficit in patients with ON **(Cao et al., 2011)**. Therefore, it is of interest to determine whether our optimized visual-noise-based CS test can measure selective MC CS deficits in patients with ON. Furthermore, Cao et al. suggested that the selective MC pathway defects may be related to elevated noise within the visual pathway. The noise-based CS test developed herein provides a tool to test this hypothesis.

To this end, we will use the static and dynamic noise paradigms developed above to determine if there is indeed a selective CS deficit in the MC pathway of ON patients. Additionally, with our approach, we endeavor to determine whether a decrease in efficiency or an increase in equivalent noise is the cause of this deficit.

B. Methods

1. Subjects

10 visually normal controls and 4 subjects with ON were recruited and tested. The mean age of the controls and patients did not differ significantly ($t = -0.35$, $p = 0.73$). The ON patients were recruited from neuro-ophthalmology clinic at the University of Illinois at Chicago and all underwent a comprehensive eye exam, including examination of the fundus and optic nerve. Characteristics of the controls and patients including age, acuity, and HVF score are given in Table 3 below. Two of the four ON patients had MS. The other two did not; they had ON due to other immunological disease.

Subject	Group	Age	MS	Acuity	HVF Score	PR-CS
□ ON 1	ON	49	Yes	0.12	-19.35	1.95
● ON 2	ON	49	No	0.24	-6.00	1.50
◆ ON 3	ON	24	Yes	0.10	-2.07	1.80
○ ON 4	ON	47	No	-0.04	0.01	1.95
Control 1	Normal	27	No	0		1.95
Control 2	Normal	27	No	-0.04		1.95
Control 3	Normal	34	No	-0.08		1.95
Control 4	Normal	37	No	-0.10		1.95
Control 5	Normal	37	No	-0.10		1.95
Control 6	Normal	38	No	-0.06		1.95
Control 7	Normal	39	No	-0.06		1.95
Control 8	Normal	39	No	-0.02		1.95
Control 9	Normal	58	No	-0.10		1.95
Control 10	Normal	62	No	-0.04		1.80

Table 3. Subject characteristics for ON patients and controls, including age, acuity, HFV scores and Pelli-Robson CS score.

2. <u>Apparatus and Procedure</u>

The apparatus and stimuli are described in the Main Methods section. Contrast threshold for letter identification was measured using letters from the Sloan set. The letter size was equivalent to 1.8 log MAR (similar to the letter size used for the Pelli-Robson CS chart). Letters were presented for a 200 ms duration against either a static (unchanging) or dynamic (changing

every 10 ms) additive white luminance noise field that had a mean luminance of 50 cd/m^2. CT for the letter stimuli was measured in noise fields that had RMS values of 0.00, 0.01, 0.03, 0.06, and 0.16. For each 20 minute testing session, data were obtained under both the static and dynamic noise paradigms for each noise RMS value.

3. Analysis

As mentioned in the Background section (Section F, page 17), the LAM can be used to model human visual performance in noise **(Legge et al., 1987 and Pelli and Farell, 1999).** In Aim 5, CT will be measured for different noise powers, allowing for plots of CT versus noise power (N), to be generated. Eq. 12, below, is the form of the LAM that will be used to fit the plots of log contrast threshold energy (E_t) versus log noise power. This allows for the derivation of k (efficiency) and N_{eq}, (equivalent internal noise). Parameters k and N_{eq} were adjusted to minimize the mean squared error between the data and the fits.

$$\log E_t = \log(k) + \log(N + N_{eq}) \qquad (12)$$

C. Results

Fig. 16 plots log contrast threshold energy E_t versus log noise power (deg^2) for the four ON patients in static noise (each ON patient is represented by a different symbol that corresponds to that given in the table above). The range of normal E_t obtained from the 10 controls is denoted by the solid light blue box. In general, all subjects had the same pattern of data, characterized by thresholds that were independent of noise power at low values of N and increasing threshold at high values of N. Three of the four ON patients had threshold elevations or were at the upper limit of normal in the absence of noise (leftmost data points). In the highest level of noise (rightmost data points) three of the four were within the normal range, with the exception of subject ON1, who had a threshold elevation for the high noise level. The pattern of

elevated threshold in the absence of noise and normal threshold in the presence of noise suggests that the curves are shifted up and rightward by similar amounts, which generally corresponds to an internal noise elevation. In contrast to the other patients, the data of Subject ON1 are shifted uniformly upward, which generally corresponds to a decrease in efficiency. Thus, somewhat different patterns of abnormality were observed among the four patients.

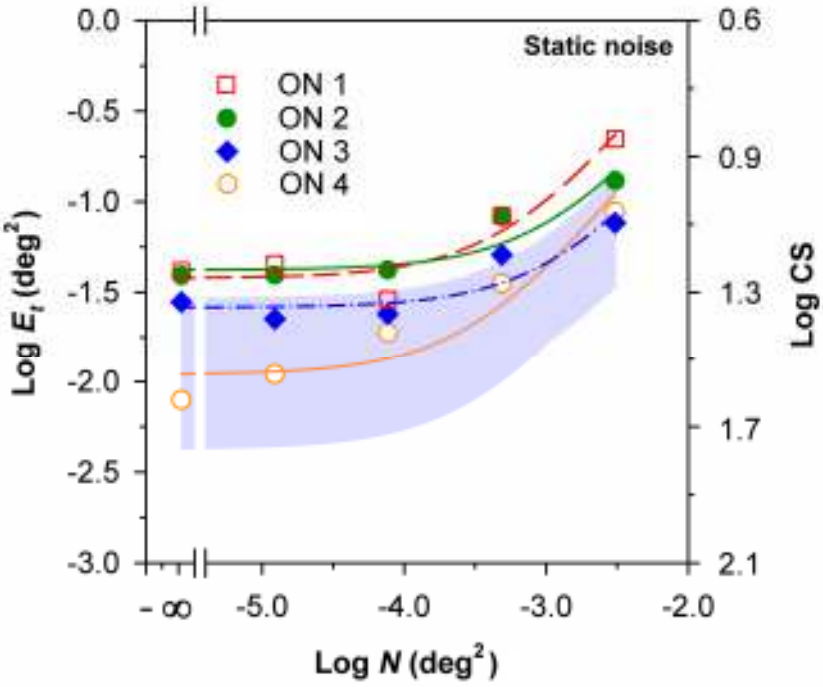

Fig 16, Log threshold energy versus log noise power for the four ON patients in static noise, log CS is shown on the right y-axis. Light blue area denotes the control range. The solid lines are the fits of Eq. 12 to the data.

Fig 17 plots log threshold energy versus log noise power for the four ON patients measured in dynamic noise. The normal range of E_t for the 10 normal subjects is denoted by the solid light blue box. In general, all subjects had the same pattern of data as observed for the

measurements in static noise, with constant threshold for low noise power and increasing threshold for high noise power. Three of the four ON patients had threshold elevations or were at the upper limit of normal in the absence of noise (leftmost data points). In the highest level of noise (rightmost data points) three of the four were within the normal range, with the exception of subject ON2 who had a threshold elevation for the highest noise level. Consistent with the findings in static noise, this pattern of findings generally corresponds to an internal noise elevation. Interestingly, patient ON2 had somewhat worse performance relative to normal in the highest noise levels compared to the lowest noise level. For this patient, the addition of noise exacerbated the CT elevation. Thus, somewhat different patterns of abnormality were observed among the four patients in dynamic noise.

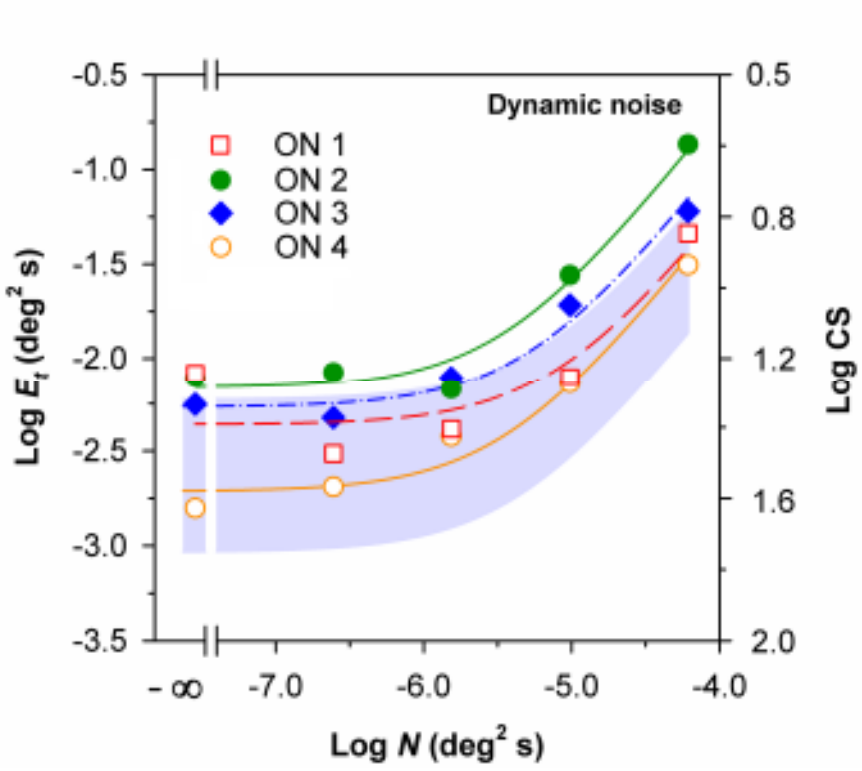

Fig 17, Log threshold energy versus log noise power for four the ON patients in dynamic noise. Other conventions are as in Fig. 16.

To better illustrate the CS abnormalities, log CS for the four ON patients is shown in no noise, and in the highest levels of static and dynamic noise in Fig. 18, below. Measurements using the standard clinical Pelli-Robson CS chart are also shown. The X's denote measurements for the control subjects and the gray boxes represent the 10^{th} to 90^{th} percentile of the control range. For the Pelli-Robson CS values, three of the four patients had normal values; the control and patient CS values did not differ significantly ($p=0.068$). For the no noise condition, two of the four patients fell below the 10^{th} percentile of the control range and one was borderline abnormal. However, the patient and control no noise CS values did not differ significantly, likely due to the small sample size ($p=0.089$). For the static noise condition, only 1 patient fell below the 10^{th} percentile of the control range, one patient was borderline abnormal, and there was a borderline statistically significant difference in mean CS between the patient and controls ($p=0.062$). For the dynamic noise condition, only 1 patient fell below the 10^{th} percentile of the control range and one patient was borderline abnormal, but the mean difference between the patients and controls did reach statistical significance ($p=0.042$).

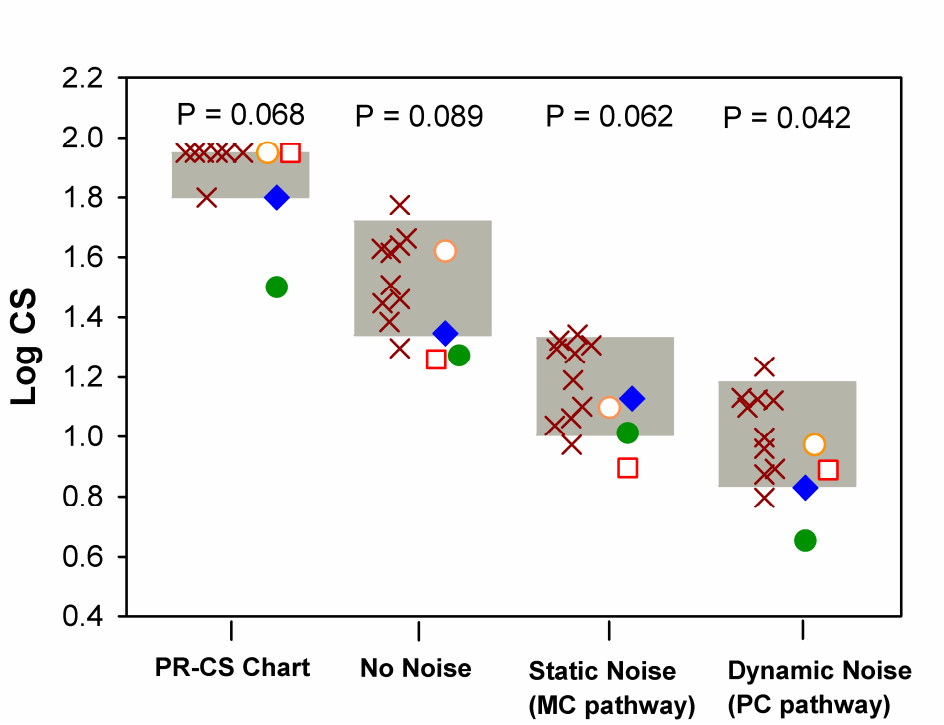

Fig 18, Log CS plotted for four ON patients in no noise, static noise and dynamic noise. PR CS is also plotted. Gray boxes denote the 10th to 90th percentile of the control data. Red X's represent the measurement for each control subject.

Based on Eq. 11 and the data shown in Fig. 16 and 17, N_{eq} was derived for each subject and is shown in Fig. 19, below. For the static noise condition, two patients had slightly elevated N_{eq} (above 90th percentile of the control group) and one patient had somewhat reduced N_{eq} (overall, there was no significant difference in mean N_{eq} between the patients and controls, p =0.951). For the dynamic noise measurements, two of the four patients were within the range of normal, two were borderline abnormal, and the mean N_{eq} for the patients and controls did not differ significantly (p= 0.458).

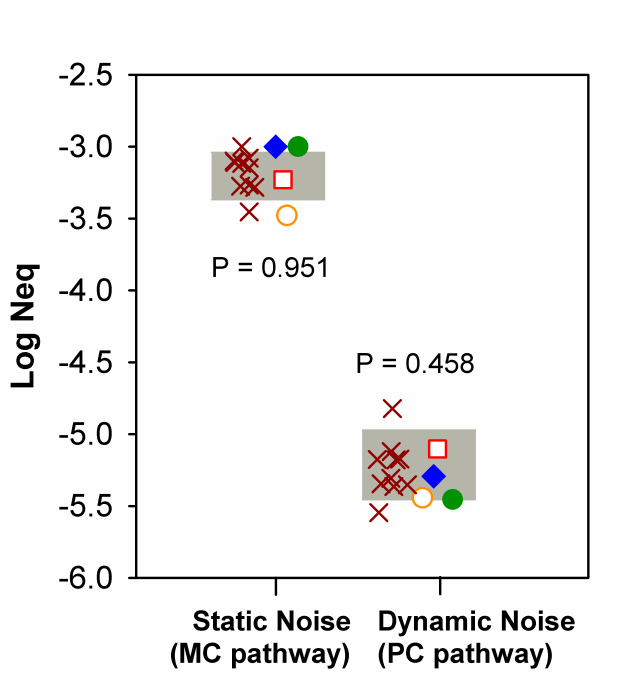

Fig 19, Log N_{eq} plotted for the four ON patients measured in static noise (left) and dynamic noise (right). Other conventions are as in Fig. 18.

Based on Eq. 11 and the data shown in Figs 16 and 17, *k* was derived for each subject, converted to efficiency and is shown in Fig. 20. For the static noise condition, the efficiency for subject ON1 was reduced below the control range and two other patients (ON2 and ON4) fell at the lower range of normal. For the dynamic noise condition, the efficiency values were clustered near the lower limit of normal and of two of the four patients fell outside of the control range. However, there were no significant differences in efficiency for this small sample in either static or dynamic noise.

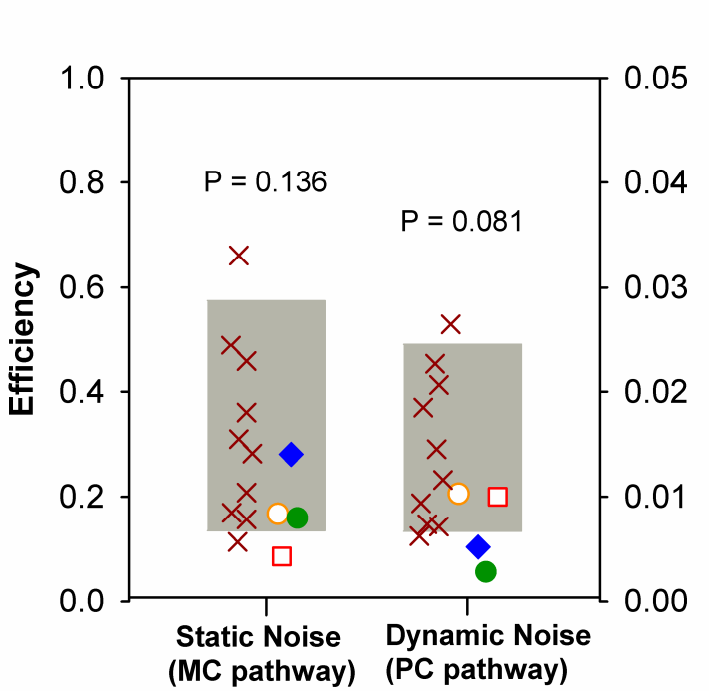

Fig. 20, Efficiency plotted for four ON patients in static noise and dynamic noise. The static noise efficiency is plotted with respect to the left y-axis and the dynamic efficiency is plotted with respect to the right y-axis.

D. Discussion

The goal of the present Aim was to provide preliminary evidence for the utility of the visual-noise-based test of letter CS developed in this thesis. To this end, measurements of CS in various levels of static and dynamic noise, and in the absence of noise, were made in visually-normal subjects and in patients who have ON. From these measurements, estimates of internal noise and efficiency were derived. Although only a small sample of data from patients with ON was obtained, some general findings can be summarized:

1) The patients' Pelli-Robson CS was normal (with one exception) and therefore Pelli-Robson CS may not be an ideal test of CS in these patients.

2) The patients' N_{eq} values were normal in dynamic noise and there were no consistent N_{eq} abnormalities in static noise.
3) The patients generally had low efficiency, some falling out of the normal range.

Although only four patients were tested, these patients spanned the spectrum of clinical dysfunction. ON4 was in the chronic phase and had normal visual acuity, no field defect, and normal Pelli-Robson CS. ON1 fell at the other end of the spectrum: mild visual acuity loss, a substantial visual field detect, but normal Pelli-Robson CS. ON3 and ON2 fell in between, having mild to moderate visual acuity loss and field defects. Interestingly, only ON2 had abnormally low PR CS, indicating that this test may not be particularly useful in these patients. In contrast to the relatively poor ability of the Pelli-Robson CS chart to separate the patient and control groups, our visual-noise-based paradigms showed abnormalities in all of the four patients. ON1 had reduced CS in the absence of noise, in the highest levels of static and dynamic noise, as well as an efficiency loss in static noise. Patients ON2 and ON3 had slightly elevated internal noise assessed by the static noise paradigm and reduced efficiency in dynamic noise. ON4 performed normally on almost all tests administered (including the standard clinical assays). Surprisingly, this patient had a lower N_{eq} than all of the controls in static noise. However, the fit of Eq. 12 to the data was poor (Fig. 16), and N_{eq} maybe have been underestimated. Note also that ON4 had thresholds near the lower limit of normal in the absence of noise, and near the upper limit of normal in the highest level of static noise.

Although the data are promising, a larger number of patients must be tested to identify consistent trends. Importantly, future samples will need to contain a larger number of subjects within the different phases of the disease, as the different model parameters may be more or less

normal at different stages. In sum, the data from this Aim serve as a proof of concept that the noise-based letter CS test may be useful and that the test compares favorably with current tests.

IX. SUMMARY OF MAIN FINDINGS

In Aim 1, we determined that using all 10 letters of the Sloan letter set was a reasonable choice for letter CS testing. We then determined in Aim 2 that the MC pathway mediates CS under the static noise condition, whereas the PC pathway mediates CS for the dynamic noise condition at high noise power. In Aim 3, we determined that letter sizes of 1.4 log MAR or larger were best suited to target the MC and PC pathways. We also found that the static noise condition was similar to the steady-pedestal paradigm in that it targets the MC pathway, and the dynamic noise condition was similar to the pulsed-pedestal paradigm because it targets the PC pathway. In Aim 4, we determined that the noise-based letter CS test is able to target the MC and PC pathways across a broad range of duration. And finally, in Aim 5, we demonstrated proof-of-concept for our test in examining the internal noise and efficiency for patients with ON. Future work is needed to evaluate MC and PC pathway CS in patients who have ON, but the data obtained in the present thesis suggest that visual-noise-based letter CS tests may be useful in this population.

X. REFERENCES

Alexander, Kenneth R., Deborah J. Derlacki, and Gerald A. Fishman. "Contrast thresholds for letter identification in retinitis pigmentosa." Investigative Ophthalmology & Visual Science 33.6 (1992): 1846-1852.

Alexander, Kenneth R., Wei Xie, and Deborah J. Derlacki. "Spatial-frequency characteristics of letter identification." Journal of the Optical Society of America A 11.9 (1994): 2375-2382.

Alexander, Kenneth R., Wei Xie, and Deborah J. Derlacki. "Visual acuity and contrast sensitivity for individual Sloan letters." Vision Research 37.6 (1997): 813-819.

Alexander, Kenneth R., Joel Pokorny, Vivianne Smith, Gerald Fishman, and Claire Barnes. "Contrast discrimination deficits in retinitis pigmentosa are greater for stimuli that favor the magnocellular pathway." Vision Research 41.5 (2001): 671-683.

Alexander, Kenneth R., Claire S. Barnes, Gerald A. Fishman, Joel Pokorny, and Vivianne Smith. "Contrast sensitivity deficits in inferred magnocellular and parvocellular pathways in retinitis pigmentosa." Investigative Ophthalmology & Visual Science 45.12 (2004): 4510-4519.

Alexander, Kenneth R., Claire S. Barnes, and Gerald A. Fishman. "Characteristics of contrast processing deficits in X-linked retinoschisis." Vision Research 45.16 (2005): 2095-2107.

Alexander, Kenneth R., and J. Jason McAnany. "Determinants of contrast sensitivity for the tumbling E and Landolt C." Optometry and Vision Science: Official Publication of the American Academy Of Optometry 87.1 (2010): 28.

Allard, Rémy, and Patrick Cavanagh. "Crowding in a detection task: External noise triggers change in processing strategy." Vision Research 51.4 (2011): 408-416.

Anderson, Roger S., and Larry N. Thibos. "Sampling limits and critical bandwidth for letter discrimination in peripheral vision." Journal of the Optical Society of America A 16.10 (1999): 2334-2342.

Anderson, Roger S., and Larry N. Thibos. "The filtered Fourier difference spectrum predicts psychophysical letter discrimination in the peripheral retina." Spatial Vision 17.1 (2004): 5-15.

Arden, G. B. "Doyne Memorial Lecture, 1978. Visual loss in patients with normal visual acuity." Transactions of the Ophthalmological Societies of the United Kingdom 98.2 (1978): 219.

Balcer, Laura J. "Optic neuritis." New England Journal of Medicine 354.12 (2006): 1273-1280.

Banks, Martin S., Wilson S. Geisler, and Patrick J. Bennett. "The physical limits of grating visibility." Vision Research 27.11 (1987): 1915-1924.

Barlow, Horace B. "Retinal noise and absolute threshold." Journal of the Optical Society of America 46.8 (1956): 634-639.

Bennett, Patrick J., Allison B. Sekuler, and Linda Ozin. "Effects of aging on calculation efficiency and equivalent noise." Journal of the Optical Society of America A 16.3 (1999): 654-668.

Berry, George A.. “Remarks on retro-bulbar neuritis with special reference to the condition of the light sense in that affection.” Ophthalmic Hospital Reports 12 (1889): 244-254.

Bjerrum, Jannik. "Untersuchungen über den Lichtsinn und den Raumsinn bei verschiedenen Augenkrankheiten." Albrecht von Græfe's Archiv für Ophthalmologie 30 (1884): 201-260.

Blakemore, Cohn, and Fergus W. Campbell. "Adaptation to spatial stimuli." The Journal of Physiology 200.1 (1969): 11-13.

Bondarko, Valeria M., and Marina V. Danilova. "What spatial frequency do we use to detect the orientation of a Landolt C?." Vision Research 37.15 (1997): 2153-2156.

Bouguer, Pierre. Traité d'optique sur la gradation de la lumière. 1760.

Brusa, Adriana, Stephen J. Jones, and Gordon T. Plant. "Long-term remyelination after optic neuritis." Brain 124.3 (2001): 468-479.

Bull, Ole B. "Studien über Lichtsinn und Farbensinn." Albrecht von Graefes Archiv für Ophthalmologie 27.1 (1881): 54-154.

Campbell, Fergus W., and John G. Robson. "Application of Fourier analysis to the visibility of gratings." The Journal of Physiology 197.3 (1968): 551.

Cao, Dingcai., Andrew J. Zele, Joel Pokorny, David Y. Lee, Leonard V. Messner, Christopher Diehl, and Susan Ksiazek. "Functional Loss in the Magnocellular and Parvocellular Pathways in Patients with Optic Neuritis." Investigative Ophthalmology & Visual Science 52.12 (2011): 8900.

Chung, Susana TL, Gordon E. Legge, and Bosco S. Tjan. "Spatial-frequency characteristics of letter identification in central and peripheral vision." Vision Research 42.18 (2002): 2137-2152.

Cleland, B. G., William R. Levick, and Kenneth J. Sanderson. "Properties of sustained and transient ganglion cells in the cat retina." The Journal of Physiology 228.3 (1973): 649-680.

Curcio, Christine A., Kenneth R. Sloan, Robert E. Kalina, Anita E. Hendrickson. "Human photoreceptor topography." Journal of Comparative Neurology 292.4 (1990): 497-523.

Derefeldt, Gunilla, Gunnar Lennerstrand, and Björn Lundh. "Age variations in normal human contrast sensitivity." Acta Ophthalmologica 57.4 (1979): 679-690.

Derrington, Andrew M., and Peter Lennie. "Spatial and temporal contrast sensitivities of neurones in lateral geniculate nucleus of macaque." The Journal of Physiology 357 (1984): 219.

Edmund, Carsten. "Uber Hemeralopia Idiopatica Mit Besonderem Hinblick Auf Untersuchung Und Behandlung." Acta Ophthalmologica 2.1 - 2 (1924): 225-238.

Elliott, Sarah L., and John S. Werner. "Age-related changes in contrast gain related to the M and P pathways." Journal of Vision 10.4 (2010): 4-4.

Fechner, Gustav. "Elements of psychophysics. Vol. I." (published in 1860; translated and re-published in 1966).

Ferris, Frederick L., Kassoff, A., George H. Bresnick, and Bailey, I.. "New visual acuity charts for clinical research." American Journal of Ophthalmology 94.1 (1982): 91-96.

Flanagan, Patrick, and Connie Markulev. "Spatio-temporal selectivity of loss of colour and luminance contrast sensitivity with multiple sclerosis and optic neuritis." Ophthalmic and Physiological Optics 25.1 (2005): 57-65.

Foroozan, Rod, et al. "Acute demyelinating optic neuritis." Current Opinion in Ophthalmology 13.6 (2002): 375-380.

Freedman, Ralph D., and Larry N. Thibos. "Contrast sensitivity in humans with abnormal visual experience." The Journal of Physiology 247.3 (1975): 687.

Friis, Harald T. "Noise figures of radio receivers." Proceedings of the Institute of Radio Engineers 32.7 (1944): 419-422.

Frohman, Elliot M., et al. "The neuro-ophthalmology of multiple sclerosis." The Lancet Neurology 4.2 (2005): 111-121.

Gabor, Dennis. "Theory of communication. Part 1: The analysis of information." Electrical Engineers-Part III: Journal of the Institution of Radio and Communication Engineering, 93.26 (1946): 429-441.

García-Pérez, Miguel A. "Forced-choice staircases with fixed step sizes: asymptotic and small-sample properties." Vision Research 38.12 (1998): 1861-1881.

Ginsburg, Arthur P. "A new contrast sensitivity vision test chart." Optometry & Vision Science 61.6 (1984): 403-407.

Gorea, Andrei. "A Refresher of the Original Bloch's Law Paper (Bloch, July 1885)." i-Perception 6.4 (2015): 2041669515593043.

Gualtieri, Mirella, Marcio Bandeira, Russel D. Hamer, Marcelo F. Costa, Oliveira, A. G. F., Ana L. A. Moura and Valerio Carelli. "Psychophysical analysis of contrast processing segregated into magnocellular and parvocellular systems in asymptomatic carriers of Leber's hereditary optic neuropathy." Visual Neuroscience 25.03 (2008): 469-474.

Gualtieri, Mirella, Marcio Bandeira, Russel D. Hamer, Francisco M. Damico, Ana L. A. Moura, and Dora F. Ventura. "Contrast sensitivity mediated by inferred magno-and parvocellular pathways in type 2 diabetics with and without nonproliferative retinopathy." Investigative Ophthalmology & Visual science 52.2 (2011): 1151-1155.

Hall, Cierra, Shu Wang, Reema Bhagat, and J. Jason McAnany. "Effect of luminance noise on the object frequencies mediating letter identification." Frontiers in Psychology 5 (2014).

Hall, Cierra, Shu Wang, and J. Jason McAnany. "Individual Letter Contrast Thresholds: Effect of Object Frequency and Noise." Optometry & Vision Science 92.12 (2015): 1125-1132.

Hawkins, Anjali S., et al. "Comparison of contrast sensitivity, visual acuity, and Humphrey visual field testing in patients with glaucoma." Journal of Glaucoma 12.2 (2003): 134-138.

Hess, Robert F., and Edwin R. Howell. "The threshold contrast sensitivity function in strabismic amblyopia: evidence for a two type classification." Vision Research 17.9 (1977): 1049-1055.

Huang, Changbing, Liming Tao, Yifeng Zhou, and Zong-Lin Lu. "Treated amblyopes remain deficient in spatial vision: A contrast sensitivity and external noise study." Vision Research 47.1 (2007): 22-34.

Hyvärinen, Lea, Pentti Laurinen, and Jyrki Rovamo. "Contrast sensitivity in evaluation of visual impairment due to diabetes." Acta Ophthalmologica 61.1 (1983): 94-101.

Jacoby, Roy, Donna Stafford, Nobuo Kouyama, and David Marshak. "Synaptic inputs to ON parasol ganglion cells in the primate retina." The Journal of Neuroscience 16.24 (1996): 8041-8056.

Kandel, Eric R., James H. Schwartz, and Thomas M. Jessell, eds. Principles of Neural Science. Vol. 4. New York: McGraw-Hill, 2000.

Kaplan, Ehud, Barry B. Lee, and Robert M. Shapley. "New views of primate retinal function." Progress in Retinal Research 9 (1990): 273-336.

Kersten, Daniel, Robert F. Hess, and G. T. Plant. "Assessing contrast sensitivity behind cloudy media." Clinical Vision Sciences 2.3 (1988): 143-158.

Khosla, Pradeep K., D. Talwar, and Hem K. Tewari. "Contrast sensitivity changes in background diabetic retinopathy." Canadian Journal of Ophthalmology. Journal Canadien d'Ophtalmologie 26.1 (1991): 7-11.

Kleiner, Robert C., Cheryl Enger, Marguerite F. Alexander, and Stuart L. Fine. "Contrast sensitivity in age-related macular degeneration." Archives of Ophthalmology 106.1 (1988): 55-57.

Kukkonen, Helja, Jyrki Rovamo, and Risto Näsänen. "Masking potency and whiteness of noise at various noise check sizes." Investigative Ophthalmology & Visual Science 36.2 (1995): 513-518.

Kulikowski, Janus J., and David J. Tolhurst. "Psychophysical evidence for sustained and transient detectors in human vision." The Journal of Physiology 232.1 (1973): 149.

Lee, Barry B., Joel Pokorny, Paul R. Martin, Arne Valberg and Vivianne C. Smith. "Luminance and chromatic modulation sensitivity of macaque ganglion cells and human observers." Journal of the Optical Society of America A 7.12 (1990): 2223-2236.

Lee, Barry B. "Receptive field structure in the primate retina." Vision Research 36.5 (1996): 631-644.

Leonova, Anna, Joel Pokorny, and Vivianne C. Smith. "Spatial frequency processing in inferred PC-and MC-pathways." Vision Research 43.20 (2003): 2133-2139.

Legge, Gordon E. "Sustained and transient mechanisms in human vision: Temporal and spatial properties." Vision Research 18.1 (1978): 69-81.

Legge, Gordon E., Daniel Kersten, and Arthur E. Burgess. "Contrast discrimination in noise." Journal of the Optical Society of America A 4.2 (1987): 391-404.

Levi, Dennis M., and Stanley A. Klein. "Noise provides some new signals about the spatial vision of amblyopes." The Journal of Neuroscience 23.7 (2003): 2522-2526.

Levitt, H. C. "Transformed up-down methods in psychoacoustics." The Journal of the Acoustical Society of America 49.2B (1971): 467-477.

Levine, Michael W. "Fundamentals of sensation and perception." Oxford University Press (3rd edition) (2000).

Leonova, Anna, Joel Pokorny, and Vivianne C. Smith. "Spatial frequency processing in inferred PC-and MC-pathways." Vision Research 43.20 (2003): 2133-2139.

Lindberg, C. Ronald, Gerald A. Fishman, Robert J. Anderson and Victoria Vasquez. "Contrast sensitivity in retinitis pigmentosa." British Journal of Ophthalmology 65.12 (1981): 855-858.

Manahilov, Velitchko, Julie Calvert, and William A. Simpson. "Temporal properties of the visual responses to luminance and contrast modulated noise." Vision Research 43.17 (2003): 1855-1867.

Majaj, N. J., Pelli, D. G., Kurshan, P., & Palomares, M. "The role of spatial frequency channels in letter identification." Vision Research 42.9 (2002): 1165-1184.

Masson, Antoine-Philibert. Études de photometrie électrique. Bachelier, 1845.

"MATLAB Documentation." Geometric Mean. MATLAB R2016a, n.d. Web. 14 July 2016.

Michelson, Albert Abraham. Studies in Optics. Courier Corporation, 1995.

McAnany, J. Jason. "The effect of exposure duration on visual acuity for letter optotypes and gratings." Vision Research 105 (2014): 86-91.

McAnany, J. Jason, and Kenneth R. Alexander. "Contrast sensitivity for letter optotypes vs. gratings under conditions biased toward parvocellular and magnocellular pathways." Vision Research 46.10 (2006): 1574-1584.

McAnany, J. Jason, and Kenneth R. Alexander. "Spatial frequencies used in Landolt C orientation judgments: relation to inferred magnocellular and parvocellular pathways." Vision Research 48.26 (2008): 2615-2624.

McAnany, J. Jason, and Kenneth R. Alexander. "Contrast thresholds in additive luminance noise: Effect of noise temporal characteristics." Vision Research 49.11 (2009): 1389-1396.

McAnany, J. Jason, and Kenneth R. Alexander. "Spatial contrast sensitivity in dynamic and static additive luminance noise." Vision Research 50.19 (2010): 1957-1965.

McAnany, J. Jason, Kenneth R. Alexander, Jennifer I. Lim, and Mahnaz Shahidi. "Object frequency characteristics of visual acuity." Investigative Ophthalmology & Visual Science 52.13 (2011): 9534-9538.

McAnany, J. Jason, Kenneth R. Alexander, Mohamed A. Genead, and Gerald A. Fishman. "Equivalent Intrinsic Noise, Sampling Efficiency, and Contrast Sensitivity in Patients With Retinitis Pigmentosa." Investigative Ophthalmology & Visual Science 54.6 (2013): 3857-3862.

McKendrick, Allison. M., Geoff P. Sampson, Mark J. Walland, and David R. Badcock. "Contrast sensitivity changes due to glaucoma and normal aging: low-spatial-frequency losses in both magnocellular and parvocellular pathways." Investigative Ophthalmology & Visual Science 48.5 (2007): 2115-2122.

Merigan, William H., and John HR Maunsell. "How parallel are the primate visual pathways?." Annual Review of Neuroscience 16.1 (1993): 369-402.

Mumford, William Walden, and Elmer H. Scheibe. "Noise performance factors in communication systems." (1968).

Nordmann, Jean-Philippe, Ralph D. Freeman, and Christian F. P. Casanova. "Contrast sensitivity in amblyopia: masking effects of noise." Investigative Ophthalmology & Visual Science 33.10 (1992): 2975-2985.

Oruç, Ipek, and Michael S. Landy. "Scale dependence and channel switching in letter identification." Journal of Vision 9.9 (2009): 4-4.

Parish, David H., and George Sperling. "Object spatial frequencies, retinal spatial frequencies, noise, and the efficiency of letter discrimination." Vision Research 31.7 (1991): 1399-1415.

Peli, Eli. "Contrast in complex images." Journal of the Optical Society of America A 7.10 (1990): 2032-2040.

Pelli, Denis G., and John G. Robson. "The design of a new letter chart for measuring contrast sensitivity." Clinical Vision Sciences. (1988).

Pelli, Denis G., and John A. Hoepner. "Letters in noise: A visual test chart that “bypasses” the optics." Noninvasive Assessment of the Visual System, 1989 Technical Digest Series 7 (1989): 103-106.

Pelli, Denis G., and Colin Blakemore. "The quantum efficiency of vision." Vision: Coding and Efficiency (1990): 3-24.

Pelli, Denis G., and Bart Farell. "Why use noise?." Journal of the Optical Society of America A 16.3 (1999): 647-653.

Pelli, Denis G., Dennis M. Levi, and Susana TL Chung. "Using visual noise to characterize amblyopic letter identification." Journal of Vision 4.10 (2004): 6-6.

Piper, H. "Uber die abhangigkeit des reizwertes leuchtender objekte von ihrer flachen-bezsw. Winkelgrosse." Zeitschrift fur Psychologie und Physiologie der Sinnesorgane 32 (1903): 98-112.

Põder, Endel. "Spatial-frequency spectra of printed characters and human visual perception." Vision Research 43.14 (2003): 1507-1511.

Pokorny, Joel, and Vivianne C. Smith. "Psychophysical signatures associated with magnocellular and parvocellular pathway contrast gain." Journal of the Optical Society of America A 14.9 (1997): 2477-2486.

Pokorny, Joel. "Review: steady and pulsed pedestals, the how and why of post-receptoral pathway separation." Journal of Vision 11.5 (2011): 7-7.

Purpura, Keith, Daniel Tranchina, Ehud Kaplan and Robert M. Shapley. "Light adaptation in the primate retina: analysis of changes in gain and dynamics of monkey retinal ganglion cells." Visual Neuroscience 4.01 (1990): 75-93.

Purves, Dale, George J. Augustine, David Fitzpatrick, Lawrence C. Katz, Anthony-Samuel LaMantia, James O. McNamara and S. Mark Williams, editors. Neuroscience. 2nd edition. Sunderland (MA): Sinauer Associates; 2001. Available from: http://www.ncbi.nlm.nih.gov/books/NBK10799/

Regan, D. "Low-contrast letter charts and sinewave grating tests in ophthalmological and neurological disorders." Clinical Vision Sciences 2.3 (1988): 235.

Riordan-Eva, P. "Clinical assessment of optic nerve disorders." Eye 18.11 (2004): 1161-1168.

Ross, J. E., Anthony J. Bron, and D. D. Clarke. "Contrast sensitivity and visual disability in chronic simple glaucoma." British Journal of Ophthalmology 68.11 (1984): 821-827.

Selwyn, E. W. H. "The photographic and visual resolving power of lenses. Part I: Visual resolving power." Spie Milestone Series MS 59 (1992): 10-10. (Originally published in 1948)

Schade, Otto H. "Optical and photoelectric analog of the eye." Journal of the Optical Society of America 46.9 (1956): 721-739.

Schiller, Peter H., and Joseph G. Malpeli. "Functional specificity of lateral geniculate nucleus laminae of the rhesus monkey." Journal of Neurophysiology 41.3 (1978): 788-797.

Shapley, Robert. "Visual sensitivity and parallel retinocortical channels." Annual Review of Psychology 41.1 (1990): 635-658.

Shapley, Robert M., and Dominic Man-Kit Lam, eds. Contrast Sensitivity. Vol. 5. MIT Press, 1993.

Silveira, Luiz C.L., Cezar A. Saito, Barry B. Lee, Jan Kremers, Manoel da Silva Filho, Bjorg E. Kilavik, Elizabeth S. Yamada and V. Hugh Perry. "Morphology and physiology of primate M- and P-cells." Progress in Brain Research 144 (2004): 21-46.

Sjöstrand, Johan, and Lars Frisén. "Contrast sensitivity in macular disease." Acta Ophthalmologica 55.3 (1977): 507-514.

Sloan, Louise L. "New test charts for the measurement of visual acuity at far and near distances." American Journal of Ophthalmology 48.6 (1959): 807-813.

Solomon, Joshua A., and Denis G. Pelli. "The visual filter mediating letter identification." Nature 369.6479 (1994): 395-397.

Snellen, Herman. "Test-types for the determination of the acuteness of vision." (1862).

Stavrou, Efty P., and Joanne M. Wood. "Letter contrast sensitivity changes in early diabetic retinopathy." Clinical and Experimental Optometry 86.3 (2003): 152-156.

Stromeyer III, Charles F., and Bela Julesz. "Spatial-frequency masking in vision: Critical bands and spread of masking." Journal of the Optical Society of America 62.10 (1972): 1221-1232.

Trobe, Jonathan D., Roy W. Beck, Pamela S. Moke, and Patricia A. Cleary. "Contrast sensitivity and other vision tests in the optic neuritis treatment trial." American Journal of Ophthalmology 121.5 (1996): 547-553.

Walls, Daniel. F. "Evidence for the quantum nature of light." Concepts of Quantum Optics (1983): 182.

Watson, Andrew B. "A formula for human retinal ganglion cell receptive field density as a function of visual field location." Journal of Vision 14.7 (2014): 15-15.

"Wiley Human Visual System.gif." Wikipedia. Wiley, 19 Feb. 2009. Web. 14 Sept. 2016.

Wooten, Billy R., Lisa M. Renzi, Robert Moore, and Billy R. Hammond, "A practical method of measuring the human temporal contrast sensitivity function." Biomedical Optics Express 1.1 (2010): 47-58.

Xu, Pengjing, Zhong-Lin Lu, Zhuping Qiu, and Yifeng Zhou. "Identify mechanisms of amblyopia in Gabor orientation identification with external noise." Vision Research 46.21 (2006): 3748-3760.

Yates, J. Terry, Monique J. Leys, Marc Green, Wei Huang, Judie Charlton, Janis Reed, and J. Vernon Odom. "Parallel pathways, noise masking and glaucoma detection: behavioral and electrophysiological measures." Documenta Ophthalmologica 95.3-4 (1998): 283-299.

Young, Laura K., and Hannah E. Smithson. "Critical band masking reveals the effects of optical distortions on the channel mediating letter identification." Frontiers in Psychology 5 (2014).

Zahabi, Sacha, and Martin Arguin. "A crowdful of letters: Disentangling the role of similarity, eccentricity and spatial frequencies in letter crowding." Vision Research 97 (2014): 45-51.

Zele, Andrew J., Joanne M. Wood, and Cameron C. Girgenti. "Magnocellular and parvocellular pathway mediated luminance contrast discrimination in amblyopia." Vision Research 50.10 (2010): 969-976.

Zhang, Lan, Denis G. Pelli, and John G. Robson. "The effects of luminance, distance, and defocus on contrast sensitivity as measured by the Pelli-Robson chart." Investigative Ophthalmology & Visual Science 30 (1989): 406.

Zimmern, Ronald L., Fergus W. Campbell, and I. M. S. Wilkinson. "Subtle disturbances of vision after optic neuritis elicited by studying contrast sensitivity." Journal of Neurology, Neurosurgery & Psychiatry 42.5 (1979): 407-412.

XI. APPENDICES

APPENDIX A. LETTER FILTERING EXAMPLE

```
imdir = 'C:\Documents and Settings\HardingFPA\My Documents\MATLAB\final
program\letters\';
Letter_read = imread('H.tif'); %read in letter
% imshow(Letter)

[m,n] = size(Letter_read); %get size of letter matrix, m by n
Letter = im2double(Letter_read);
Letter1 = Letter;
letter_fft = fft2(Letter1); %fft of letter
d0=2.82; %D0 is a specified nonnegative number; filter cutoff

d=zeros(m,n); %initialize zeros matrix
h=zeros(m,n); %initialize zeros matrix

[U,V] = dftuv(m,n); %compute meshgrid frequency matricies

d = sqrt(U.^2 + V.^2); %%%%% %calculate the distance from point (u,v) to the
center of the filter.

lp = exp(-(d.^2)./(2*(d0^2))); %gaussian LP filter

hp = 1 - lp; %gaussian HP filter

%%change for lp or hp the following line:
filtering = lp.*letter_fft; %letter into the filter: should be mostly black
with speckles at corners

filt_letter = ifft2(filtering); %inverse fft %% for LP
% filt_letter = ifft2(filtering-.5)+.5; %inverse fft %% for HP

imshow(filt_letter) %display filtered letter

% imwrite(filt_letter,'filt_letter.tif');
%  diff = testletterh-filt_letter
```

XII. VITA

NAME: CIERRA MICHELLE HALL

EDUCATION:

B.S.	**Bioengineering, University of Illinois at Chicago**	**2006-2011**
Ph.D.	**Bioengineering, University of Illinois at Chicago**	**2011-2016**

RESEARCH EXPERIENCE:

- **Graduate Research Assistant** under PI and Professor Jason McAnany, University of Illinois at Chicago, Dept of Ophthalmology and Bioengineering, 8/12 – 12/16
    - Investigator 101 and HIPAA certified

- **Graduate Research Assistant** under Professor Anjum Ansari, University of Illinois at Chicago Dept. of Physics and Bioengineering, 5/11 - 9/12

- **Undergraduate Research / Paid Research Assistant** under Professor Andreas Linninger, University of Illinois at Chicago, 12/09 - 4/11

- **NSF Research Experience for Undergraduates** under Professor Andreas Linninger, University of Illinois at Chicago, Summer 2010

NON ACADEMIC WORK EXPERIENCE:

- **Graduate Assistant to Agreement Specialist** under Heather Claxton-Douglas, University of Illinois at Chicago, Office of Technology Management, 8/16 – 12/16
    - Worked with Sophia system

- **Office Manager** under Ray Comas, CSW Solutions, Chicago, IL, 9/08 – 10/09

- **Administrative Assistant and Bookkeeper** under Howard Hammond, H&H Press, Chicago, IL, 4/08 – 1/09

PUBLICATIONS:

- **Cierra Hall**, Shu Wang, J. Jason McAnany. Individual Letter Contrast Thresholds: Effect of Object Frequency and Noise. *Optometry & Vision Science*. 2015.

- **Cierra Hall**, Shu Wang, Reem Bhagat and J. Jason McAnany. Effect of luminance noise on the object frequencies mediating letter identification. *Frontiers in Psychology*. 2014.

- Andrej Mošat', Eric Lueshen, Martina Heitzig, **Cierra Hall**, Andreas A. Linninger, Gürkan Sin, Rafiqul Gani. First principles pharmacokinetic modeling: A quantitative study on Cyclosporin. *Computers and Chemical Engineering*. 2013.

- **Cierra Hall**, Andrej Mošať, Eric Lueshen, and Andreas A. Linninger. Interspecies Scaling in Pharmacokinetics: A Novel Whole Body Physiologically-Based Modeling Framework to Discover Drug Biodistribution Mechanisms In Vivo. *Journal of Pharmaceutical Sciences.* 2012.

POSTERS:

- **VSS 2016, Tampa, Florida, 5/16**

Poster: *Temporal characteristics of luminance noise affect the pathway mediating contrast sensitivity.* Cierra Hall, J Jason McAnany.

- **UIC College of Medicine Research Forum 2015, Chicago, IL, 12/15**

Poster: *A novel, noise-based test of letter contrast sensitivity.* Cierra Hall, J Jason McAnany.

- **ARVO 2014, Orlando, Florida, 5/14**

Poster: *Effect of luminance noise on contrast threshold for individual Sloan letters.* Cierra Hall, Reema Bhagat, Shu Wang, J Jason McAnany.

- **Computers & Chemical Engineering 2013 Best Paper Award Winner**

Paper: Andrej Mošat', Eric Lueshen, Martina Heitzig, **Cierra Hall**, Andreas A. Linninger, Gürkan Sin, Rafiqul Gani. *First principles pharmacokinetic modeling: A quantitative study on Cyclosporin*. Computers and Chemical Engineering. 2013

- **Gordon Research Conference on Biopolymers, Newport, RI, 5/12**

Poster: *DNA-bending and base-flipping dynamics during lesion recognition by XPC.* Yogambigai Velmurugu, Xuejing Chen, Cierra Hall, Jung-Hyun Min, and Anjum Ansari.

- **AICHE National Meeting, Salt Lake City, Utah, 11/10**

Poster: 2nd Place Honorable Mention with over 70 contestants, CAST Director Award: *Parameter Estimation In Global Pharmacokinetic Models for Drug Delivery*. Andrej Mošat, Eric Lueshen, Cierra Hall and Andreas A. Linninger.

Speech: *Parameter Estimation In Global Pharmacokinetic Models for Drug Delivery*. Andrej Mošať, Eric Lueshen, Cierra Hall and Andreas A. Linninger.

Speech: *Model Based Quality by Design in Drug Substance or Drug Product*. Andrej Mošať, Eric Lueshen, Cierra Hall and Andreas A. Linninger.

- **Midwest Bioengineering Career Conference 2011, Evanston, Illinois, 4/11**

Poster: **1st place** out of approximately 25 contestants. *Pharmacokinetic Scaling and Discovery of In Vivo Drug Distribution Mechanisms with a Novel Whole-Body*

Physiologically-Based Modeling Framework. Cierra Hall, Eric Lueshen, Martina Heitzig, Andreas Linninger.

- **UIC College of Engineering Senior Design Exposition, Chicago, IL, 4/11**

Poster: **1st Place** in the *Medical Devices* category. *Rational Design of a Decision-Making Tool for Brain Surgeons*. Nicholas Vaičaitis, Brian Henry, Cierra M. Hall and Andreas A. Linninger.

- **21st European Symposium on Computer Aided Process Engineering Thessaloniki, Greece, 5/11**

Poster: Eric Lueshen, Cierra Hall, Andrej Mošaťand Andreas Linninger. *Physiologically-Based Pharmacokinetic Modeling: Parameter Estimation for Cyclosporin A*.

HONORS AND AWARDS:

- **Board of Trustees Tuition and Fee Wavier**, full tuition and fees sponsored by the Board of Trustees, Spring 2016

- **CCTS PECTS Fellowship**, 1 year of full tuition and fees sponsored by the UIC College of Medicine, 8/15-8/16

- **UIC Student Travel Presenter's Award**: $100, 5/14 & 5/16

- **GSC Student Travel Award**: $275, 4/14, 5/16

- **Computers & Chemical Engineering, 2013 Best Paper Award Winner**

Paper: Andrej Mošat', Eric Lueshen, Martina Heitzig, **Cierra Hall**, Andreas A. Linninger, Gürkan Sin, Rafiqul Gani. First principles pharmacokinetic modeling: A quantitative study on Cyclosporin. *Computers and Chemical Engineering*. 2013

TEACHING EXPERIENCE:

- **TA** for Prof. Mike Muller's BIOS 100 course, *Biology of Cells and Organisms*, 1/15-5/15
- **TA** for Prof. Hananeh Esmailbeigi's BIOE 431 course, *Bioinstrumentation and Measurement Laboratory*, 1/14-5/14

- **TA** under Dr. Andy Tillotson for PHYS 106 course, *Introductory Physics*, 1/12-5/13 (2 semesters)

- **TA** for Prof. James Patton's BIOE 431 course, *Bioinstrumentation and Measurement Laboratory*, 1/12-5/12

- **TA** under Professor Miiri Kotche for BIOE 101 course, *Introduction to Bioengineering*, 8/11-12/11

- University of Illinois at Chicago, IL, Mathematical Sciences Learning Center, **Peer Math Tutor**, 1/07-5/07

ACADEMIC SERVICE:

- UIC College of Engineering - Student Engineering Expo, **Alumni Judge**, 4/15
- Vice Chancellor For Research - Student Research Forum, **Alumni Judge**, 4/15, 4/16
- Undergraduate Bioengineering Student Journal (UBSJ), **Editor In Chief and Associate Editor**, 1/12 – 12/16
- National Engineers Week: "Launching Tomorrow" at the Adler Planetarium Global Engineering Marathon **Panel Discussion** with Astronaut Sally Ride, 2/25/2010
- Biomedical Engineering Society (BMES) **member** – UIC Student Chapter, 8/10 – 8/12
- **Dean's List** – An Academic Acknowledgement for High Semester GPA, Spring 2009